Chapter 5

Extracellular Space and its role in neuronal signal transmission for both Healthy and Diseased Nerve Fiber

This chapter aims at developing a robust and a simplistic mathematical model of the nerve membrane potential that would include the ECS dependent parameters in order to have a holistic framework to understand neuronal signal transmission in detail. The model expands the conventional cable model by incorporating the ECS dependent parameters into the membrane potential expression. This work involves the study of neuronal signal transmission for a healthy and diseased (injured) nerve fiber. Moreover, the work also involves the understanding of how genetic mutation and other channelopathies affects signal transmission through alteration in the gating variables or rate constant and proposing a rescue protein mechanism that could alter the effects of the mutations.

5.1 Introduction

An action potential is primarily produced by the voltage-gated sodium and potassium ion channels that are found throughout the nerve fiber [18]. The voltage-gated sodium channels open in response to a stimulus that depolarizes the neuron's membrane potential which allow sodium ions (Na^+) to enter the cell quickly, increasing the membrane potential and starting the process of depolarization. At the peak of depolarization, the sodium channels inactivate stopping the further inflow of sodium ions (Na^+) and potassium ions (K^+) starts exiting the cell initiating the repolarization phase of the action potential which reduces the membrane potential back to its resting state. The coordinated activity of these ion channels ensures the accuracy of the action potential timing.

Neuronal injury can result from several events such as trauma, ischemia, neurodegenerative disorders, and exposure to toxins [166], [167], [168], [169], [170], [171]. A sequence of events are triggered when neurons are damaged and in severe circumstances this can result in cellular malfunction and neuronal death. One of the main consequences of neuronal damage is the disturbance of potassium (K^+) and sodium (Na^+) ion concentrations that are crucial for preserving the proper functioning of neurons which may attribute to condition involved in ion channel blocking or alteration to the ionic concentration which further leads to sensory or motor

impairments. Blocking of the sodium ion channels causes reduced ability of the neurons to generate an action potential while blocking of the potassium ion channels leads to prolonged duration of the action potential [98], [172], [173].

Genetic mutations of the ion channels disrupt how ion channels open and close causing disbalance to the ionic flow and sometimes leading to catastrophic consequences which may lead to a range of neurological disorders and seriously impair the nervous system's ability to send information to the intended target [19], [174], [175] . The voltage dependence of the gating variables (m, n, and h) can be altered through mutation of the sodium ion channels, especially those that are encoded by the SCN gene family (e.g., SCN1A, SCN2A, and SCN8A) because these mutations affect the rate constants that control the opening and closing of the ion channels [176], [177], [178]. These ion channel mutations lead to hyperexcitability, a disorder marked by increased neuronal activity and excessive sodium inflow [179], [180]. Diseases like epilepsy, which results in seizures caused by excessive neuronal firing, have been linked to these mutations [179], [180], for instance mutations in the SCN1A gene associated with Dravet syndrome impact sodium channels in inhibitory neurons thus reducing their ability to block excitatory signals causing frequent and severe seizures [181], [182].

Similarly, abnormalities in potassium channels, which are encoded by genes like KCNQ2, KCNA1, and KCNA2, may prevent the action potential from repolarizing [183], [184], [185] that result in delayed or obstructed ion channel opening, lowering neuronal excitation (hypoexcitation) and prolonging the refractory period. These mutations often cause shift in the voltage threshold required to activate or inactivate the ion channels which alters the gating behaviour of the ion channels. Understanding these abnormalities and their effects is crucial in developing targeted therapies that restore the normal functioning of the neurons. To mitigate the effect of these genetic mutations of the ion channels, nerve inherently possesses a rescue protein mechanism that aims to alter the effect of the genetic mutation and restore the normal neuronal excitation.

Existing literature highlights the importance of ECS in influencing neuronal signal transmission as variation in its size or diameter can lead to altered neuronal signaling [61], [62], [167]. The conventional cable model [91] of the nerve primarily focusses on the intrinsic properties of the nerve fiber to obtain a membrane potential expression. Thus, it is essential to obtain a membrane potential expression that also incorporates the fundamental parameters of the ECS to have a holistic approach towards studying neuronal signals and the current work focusses

on this very aspect of inclusion of the ECS related parameters to the membrane potential expression.

5.1.1 Rescue protein

Rescue proteins are specialised molecules that serve to restore normal cellular function by mitigating the effects of mutations which affects the ion channels of neurons [186], [187], [188], [189]. The ion channels control the movement of ions such as sodium and potassium across the cell membrane which are essential for preserving the electrical activity of nerve cells. This equilibrium may be upset by mutations in these channels, resulting in aberrant nerve signalling that may exhibit as variety of neurological disorders [190], [191].

Genetic mutation can influence the gating mechanism or change the channels response to voltage causing it to open too easily or not to open at all. A mutation may inhibit the opening of potassium channels, which results in delayed repolarization of the nerve cell, or it may cause sodium channels to remain open longer, resulting in excessive firing (hyperexcitation). In order to counteract these aberrant effects, rescue proteins engage with the mutated ion channels to either stabilize their function or restore their activity to a more normal state. This might involve altering the channel's response to variations in membrane potential or affecting their rates of opening and closing in order to effectively compensate for the mutation. These proteins help lessen or completely eradicate the negative consequences of the mutation by rescuing the normal function of the ion channels and assisting in restoring the neurons behaviour to that of a non-mutated state.

Some of the key rescue proteins are Brain-Derived Neurotrophic Factor (BDNF) and MT2 protein which are important for the growth and survival of the nerve cell especially for the retinal ganglion cells (RGC) [192] [193]. PMP22 (Peripheral Myelin Protein 22), a critical protein in the myelin sheath is vital for peripheral nerve health. Peripheral neuropathies can be brought on by mutations and treating nerve injury may result from an understanding of this rescue protein's involvement [187]. Additionally, ZBP1 is an important RNA-binding protein that ensures mRNAs are located in axons where they can be used for local protein synthesis as axons regenerate. It carries mRNAs to areas of growth and repair facilitating the prompt synthesis of proteins. ZBP1 overexpression improves regenerative capacity by overcoming growth abnormalities and its levels are necessary for neuronal injury response [188]. Hence, ZBP1 is an important target for therapeutics focused on nerve damage recovery.

However, there are instances where the rescue protein mechanism fails to counter the effect of these mutations. One important factor is the rescue protein's own deficiencies which can be brought on by improper expression, concentration, or function [194]. A mutation in the ion channels may not be able to be counteracted by the rescue protein if it is not produced in large enough amounts or if it has improper binding affinity. Another possibility is that the rescue protein is unable to reverse the structural alterations in the ion channels brought about by mutation. The physical or structural alterations in the sodium or potassium channels may be too significant for the rescue protein to rectify in such circumstances, even when it is present. This might happen if the mutation modifies the gating behaviour of the channel in a way that the rescue protein is unable to control. The capacity of the rescue protein to interact with ion channels can be impacted by environmental conditions such as variations in the pH, temperature, or ion concentration within the nerve fiber [38]. The rescue mechanism may not be able to return normal nerve excitability if these conditions are not achieved. Furthermore, the rescue protein mechanism might not work as well at certain phases of nerve injury or disease development. For instance, the nerve fiber may not react to the rescue mechanism if the mutation-induced malfunction is accompanied by degeneration or other disease processes as it is already experiencing irreversible damage. The rescue protein mechanism may fail if the protein becomes dysregulated due to a secondary mutation or issues in cellular regulation and transport. In such cases, the rescue protein might not reach the ion channels in time or function properly, leading to a failure in restoring normal nerve behaviour.

5.2 Contribution

In this work, an attempt has been made to put forward a mathematical model of the nerve membrane potential that is both simple and robust, capable of accurately mimicking the functioning of a nerve fiber and also incorporates the fundamental parameters related to the ECS. Inclusion of the ECS related parameters into this mathematical framework or model allows for a more holistic analysis of the neuronal signal transmission. The model also involves less computational complexity, robust and could be used for rapid prototyping. The work involves an exhaustive experimentation with various combinations of the ECS related parameters and biological nerve fiber to simulate various biological circumstances which provides valuable understanding about how ECS of varied sizes could influence neuronal signal transmission for a healthy and diseased (injured) nerve fiber.

Additionally, this work attempts to investigate the potential impact of genetic mutations on neuronal excitability by mimicking alterations to the voltage sensitivity of ion channels by shifting the α and β rate constants through a positive and negative voltage shift. The purpose of this voltage shift is to illustrate the potential impact of ion channel mutation on the voltage-dependent activation and inactivation characteristics of ion channel which demonstrates how mutation that causes a positive or a negative voltage shift, may alter the shape and form of the action potential spike train. Moreover, a rescue protein mechanism has also been proposed in this chapter that could allow for a better analysis of rescue operation in bringing back the mutated spike train back to its original form. In order to represent the inhomogeneity of the ECS, here the characteristic resistance (r_e) of the ECS has been varied from 10^3 Ω/cm to 10^4 Ω/cm keeping the characteristic internal resistance (r_i) of the nerve fiber at 10^4 Ω/cm. The proposed work is aimed to contribute into the existing knowledge of how a small variation in the channel dynamics can lead to a significant physiological outcome. This framework is aimed at contributing to a deeper understanding of how small changes in channel behaviour can have significant physiological consequences through a robust model that is mathematical and computational less complex, eventually directing the development of targeted treatments and strategies for associated health issues.

5.3 Proposed Methodology

For the proposed model, the well-known Rall's equivalent cable model of nerve[91] is considered, as seen in Fig.5.1 and the Hodgkin-Huxley (H-H) [17] active nerve model serves as the inspiration of the individual tank circuit which is shown in Fig.5.2. In order to have a robust approach, the parameters pertaining to the ECS such as its resistance, length and the diameter have been integrated into the model which is inspired from [75]. Since calcium currents have little to no direct influence on gating dynamics, thus it has been neglected in the study. However, for a model that involve neurotransmitter release or synaptic connection, the calcium dynamics should be taken into consideration. Using Kirchoff's Voltage Law, the corresponding internal and external voltage expression can be shown as,

$$\frac{\partial V_i}{\partial x} = -R_i I_i(x) \tag{5.1}$$

$$\frac{\partial V_e}{\partial x} = R_e I_e(x) \tag{5.2}$$

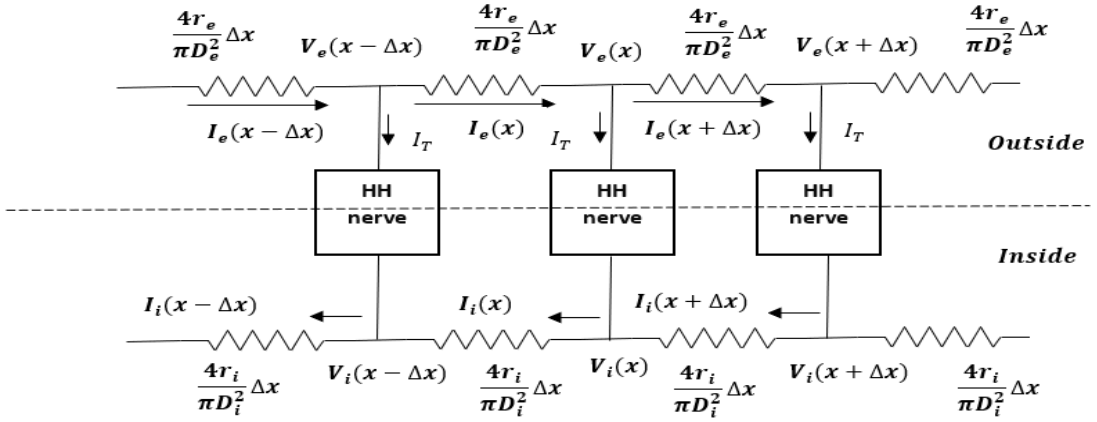

Fig.5.1 Representation of a nerve fiber by a cable

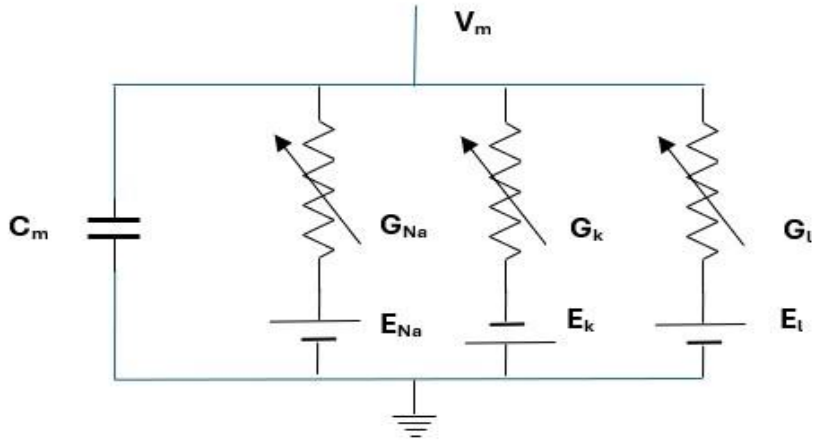

Fig.5.2 Hodgkin-Huxley (H-H) active nerve

Subtracting Eq.5.2 by Eq.5.1 gives the transmembrane voltage expression which is,

$$\frac{\partial V_m}{\partial x} = -I_a(R_e + R_i) \tag{5.3}$$

Here, I_a and V_m are the axial current and the resting membrane potential respectively. The axial resistance (R_a) is represented as the the sum of volumetric internal resistance (R_i) of the fiber and the volumetric ECS resitance (R_e). Again, the volumetric ECS resistance and the internal resistaance of the fiber can be further expanded as $R_e = \frac{4r_e}{\pi {D_e}^2}\Delta x$ and $R_i = \frac{4r_i}{\pi {D_i}^2}\Delta x$ [97]. Where, D_e and D_i are the diameter of the ECS and that of the nerve fiber respectively.

Similarly, by applying Kirchoff's current law, the transmembrane current I_T thus obtained is found to be $\frac{\partial I_a}{\partial x}$. Now, differentiating Eq.5.3 with respect to x gives,

$$\frac{\partial^2 V_m}{\partial x^2} = -\frac{\partial I_a}{\partial x}(R_e + R_i) \tag{5.4}$$

Hence, replacing $\frac{\partial I_a}{\partial x}$ by the transmembrane current I_T gives,

$$\frac{\partial^2 V_m}{\partial x^2}\left(\frac{1}{R_e + R_i}\right) = -I_T \tag{5.5}$$

Moreover, the transmembrane current (I_T) can be represented from the active H-H membrane equation as,

$$I_T = C_m \frac{\partial V_m}{\partial t} + I_{Na} + I_k + I_l \tag{5.6}$$

In Eq.5.6, the volumetric membrane capacitance is (C_m) that can be further expanded in terms of its characteristic membrane capacitance (c_m) as $C_m = c_m \pi D_i l$ and I_{Na}, I_k, and I_l are the sodium current, potassium current and leakage current respectively. According to Hodgkin-Huxley, the ionic currents can be further expanded as,

$$I_{Na} = G_{Na}(V_m - E_{Na}) \tag{5.7}$$

$$I_k = G_k(V_m - E_k) \tag{5.8}$$

$$I_l = G_l(V_m - E_l) \tag{5.9}$$

Here, G_{Na}, G_k and G_l are the sodium ion, potassium ion, and leakage ion conductance's and E_{Na}, E_k and E_l are the equilibrium potential of sodium ion, potassium ion and leakage ion respectively. The potassium conductance (G_k) takes the form of $g_k n^4$, in which g_k stands for the maximum potassium conductance and n is the potassium activation variable. Similarly, the sodium conductance (G_{Na}) can be expressed as $g_{Na} m^3 h$, where g_{Na} is the maximum sodium conductance and m^3 and h are the sodium activation and inactivation state variables respectively. Furthermore, the gating variable parameters for an active nerve fiber can be expressed as,

$$\frac{dn}{dt} = \propto_n (V_m)(1 - n) - \beta_n(V_m)n$$

$$\frac{dm}{dt} = \propto_m (V_m)(1 - m) - \beta_m(V_m)m$$

$$\frac{dh}{dt} = \propto_h (V_m)(1 - h) - \beta_h(V_m)h,$$

The rate constants $\propto_i$ and β_i for the i-th ion channel depend on voltage but are independent of time. The gating variables n, m, and h are dimensionless which ranges from 0 to 1 and are described by Boltzmann equations as functions of the membrane potential. Hodgkin and Huxley has defined the equations for the rate constants (α and β) as,

$$\propto_n (V_m) = \frac{0.01(V_m+50)}{1-\exp\left(\frac{V_m+50}{-10}\right)}, \qquad \propto_m (V_m) = \frac{0.1(V_m+35)}{1-\exp\left(\frac{V_m+35}{-10}\right)} \qquad \propto_h (V_m) = 0.07\exp\left(\frac{V_m+60}{-20}\right),$$

$$\beta_n(V_m) = 0.125\exp\left(\frac{V_m+60}{-80}\right) \qquad \beta_m(V_m) = 4\exp\left(\frac{V_m+60}{-18}\right), \qquad \beta_h(V_m) = \frac{1}{1+\exp\left(\frac{V_m+30}{-10}\right)} \quad (5.10)$$

Now, combining Eq.5.5 and Eq.5.6, the resultant expression obtained is,

$$\frac{\partial^2 V_m}{\partial x^2} + [C_m(R_e + R_i)\frac{\partial V_m}{\partial t} + (R_e + R_i)G_{Na}(V_m - E_{Na}) + (R_e + R_i)G_k(V_m - E_k) + (R_e + R_i)G_l(V_m - E_l)] = I_{inj} \quad (5.11)$$

Here, I_{inj} is the injected current. Now, considering the fiber to be equipotential then, $\frac{\partial V_m}{\partial x} = 0$, and hence, Eq.5.11 can be rewritten as,

$$[C_m(R_e + R_i)\frac{\partial V_m}{\partial t} + (R_e + R_i)G_{Na}(V_m - E_{Na}) + (R_e + R_i)G_k(V_m - E_k) + (R_e + R_i)G_l(V_m - E_l)] = I_{inj} \quad (5.12)$$

Representing Eq.5.12 in terms of ionic current gives,

$$\partial V_m = \frac{\partial t}{C_m(R_e+R_i)}[I_{inj} - (R_e + R_i)(I_{Na} + I_k + I_l)] \quad (5.13)$$

Eq.5.13 gives the membrane potential expression where the ECS related parameters have been incorporated into the model. The axial resistance which is a combination of the volumetric ECS resistance and the volumetric internal resistance of the fiber (R_e+R_i) provides for the incorporation of the ECS related term into the final membrane potential expression. The proposed model is unique in that it provides a holistic and a robust framework for studying neuronal signal transmission by successfully integrating the ECS dependent characteristics into the membrane potential expression.

5.4 Simulation Considerations

The length (l) of the fiber considered is 80 μm. The length is so considered because it strikes a balance between computing efficiency, biological realism, and accurate signal propagation dynamics modelling. Small axons, and fine neuronal branches typically fall within this range,

which guarantees that the model can faithfully capture physiological behaviour while also being computationally viable [151], [152]. The diameter of the fiber and the diameter of the ECS are 5 µm and 50 nm respectively and the resting membrane potential is -60 mV. The sodium conductance (g_{Na}), potassium conductance (g_k) and leakage conductance (g_l) are 120 Siemens/cm^2, 36 Siemens/cm^2, and 0.0003 Siemens/cm^2 respectively. The characteristic membrane capacitance (c_m) is 1 µF/cm^2. The equilibrium potential of sodium ion (E_{Na}), potassium ion (E_k) and leakage ion (E_l) are 55 mV, -72 mV, and -49 mV respectively. Putting the values in Eq.5.13 gives a relation between the membrane potential and the ECS related parameters such as its resistance (R_e) and the diameter of the ECS (D_e) according to relation $R_e = \frac{4r_e}{\pi {D_e}^2}\Delta x$. The relationship gives a membrane potential expression for an active nerve fiber in which the ECS related parameters are incorporated. The incorporation of ECS related parameters provides a holistic approach towards understanding neuronal signal transmission in a detailed manner.

5.5 Results and Discussions

The study explores the impact of nerve fiber injuries or diseases on the transmission of neuronal signals. under the influence of a varying ECS. The study also explores the effects of genetic mutations that alter the ion channels in nerve fibers, examining how these changes may interfere with regular neuronal function. The study proposes a unique rescue protein strategy to address these disturbances and possibly reverse the impact of these genetic mutations. This process provides a theoretical foundation for repairing damaged ion channels, lessening their detrimental effects on the transmission of nerve signals. The membrane potential equation for an active nerve fiber has been proposed as most of the available mathematical models does not incorporate the ECS dependent parameters, and as understood, ECS has a significant role in influencing neuronal signals. Furthermore, the Rescue protein mechanism in terms of a mathematical equation is proposed so that the amount of rescue established could be understood in a more detailed manner. Moreover, the mathematical equation is robust and involves less computational and mathematical complexities.

5.5.1 Effect of injury (diseases) on neuronal signal

A. Spike train for a healthy nerve fiber

Initially the nerve fiber is considered to be healthy i.e., it is devoid of any disease or injury and a spike train is generated as shown in Fig.5.3 for the duration of 0-12 mSec with the size of the ECS considered is 50 nm, the internal diameter of the fiber is considered to be 5 µm and the length of the fiber under consideration is 80 µm respectively. From Fig.5.3, it can be seen that

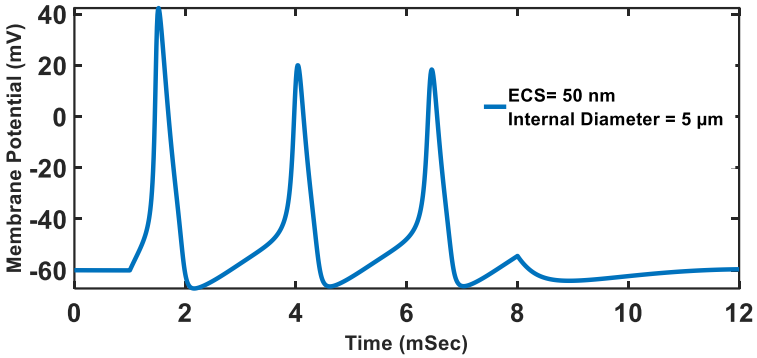

Fig.5.3 Normal Spike Train

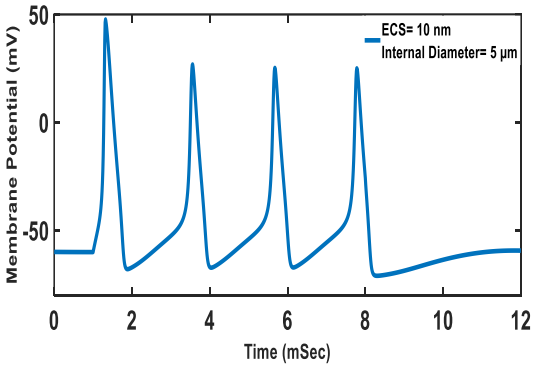

Fig.5.4 Spike Train for a smaller ECS

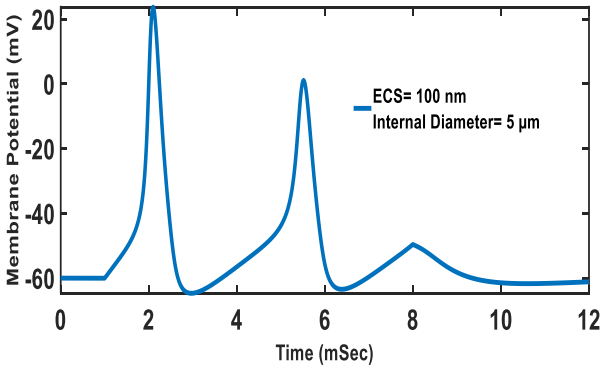

Fig.5.5 Spike Train for a larger ECS

the initial spike has an amplitude of about 42.34 mV and the amplitudes of the subsequent spikes are 20.02 mV and 18.37 mV, respectively which are somewhat lesser. This occurs due to the effects of inability of the fiber to reset after refractory period, non-recovery of the sodium channels after the first spike and potassium channel dynamics. Fig.5.4 shows the plot for the spike train when the size of the ECS is considered to be smaller i.e. of 10 nm and Fig.5.5 shows the plot for the spike train when the size of the ECS is considered to be larger i.e. of 100 nm. It is seen from Fig.5.4 and Fig.5.5 the neuronal signal undergoes more attenuation when the size of the ECS is larger than its smaller counterpart. This is in coherence with existing

knowledge, and it also shows that the size of the ECS is an important parameter to consider for studying neuronal signal.

It is seen from Fig.5.4 that for a smaller ECS (10 nm), the amplitude of the initial spike now raises to about 47.69 mV which is higher than for an ECS of 50 nm which can be seen from Fig.5.3 and the amplitude of the subsequent spikes of the spike train has also increased. Moreover, there is an additional spike that found to be generated suggesting hyperexcitation of the neuronal signal. This increase in signal amplitude is the result of a much greater resistance of the ECS preventing mobile ions from leaking into the external media owing to a smaller ECS. With a smaller ECS, spike encoding changes significantly and with hindrance to the mobile ions to get dissipated towards the external media, high amount of charged ions gets accumulated and gets delivered to the adjacent region which in turn leads to the occurrence of hyperexcitation within the same time frame. This kind of condition is synonymous with the occurrences of diseases like Epilepsy, Restless Legs Syndrome, Peripheral Neuropathy [195], [196], [197].

For a larger ECS (100 nm), its resistance is less thereby providing a greater mobility of ions to get dissipated towards the external media ultimately leading to a higher signal attenuation which is also observed from Fig.5.5. Here, the amplitude of the initial spike is found to be 23.75 mV, and the amplitude of the subsequent spikes likewise tends to get reduced. Because there is a greater likelihood of mobile ions dispersing into the extracellular medium, the neuronal signal attenuates more which leads to a decrease in its amplitude. Furthermore, the number of spikes also gets reduced suggesting hypoexcitation of the neuronal signal. Due to this leakage of ions, the amount of ions needed to maintain the strength of the neuronal signal diminishes, which may ultimately cause the signal to die down before it reaches its intended destination. This hypoexcitation like condition is synonymous with diseases like Guillain-Barré Syndrome, Charcot-Marie-Tooth Condition [198], [199], [200][201], [202].

B. Spike train for an injured (diseased) nerve fiber that results in the blocking or alteration of ion channels

In this section, the simulation is carried out under the assumption that the nerve fiber is injured or diseased. The concentrations of sodium and potassium ions are significantly impacted by any kind of nerve damage. The impact of neuronal damage on ion channel blocking and ion channel alternation and its subsequent effect on neuronal signal under the influence of the ECS is studied in this section.

B.1. Spike train when sodium ion channels are blocked

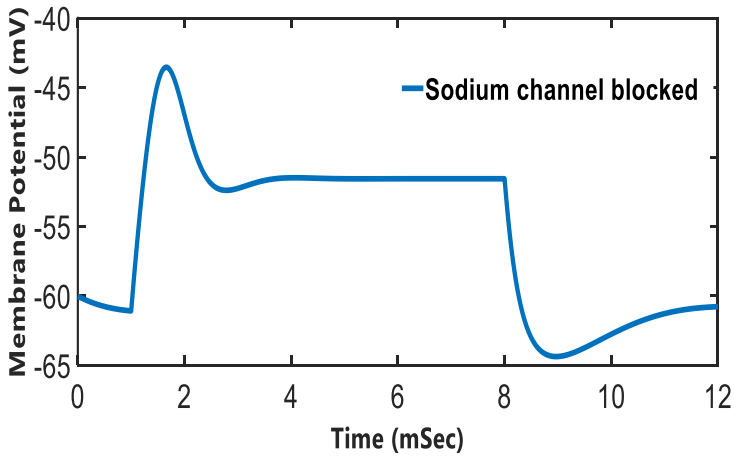

Fig.5.6 Spike Train when sodium channels are blocked, ECS= 50 nm

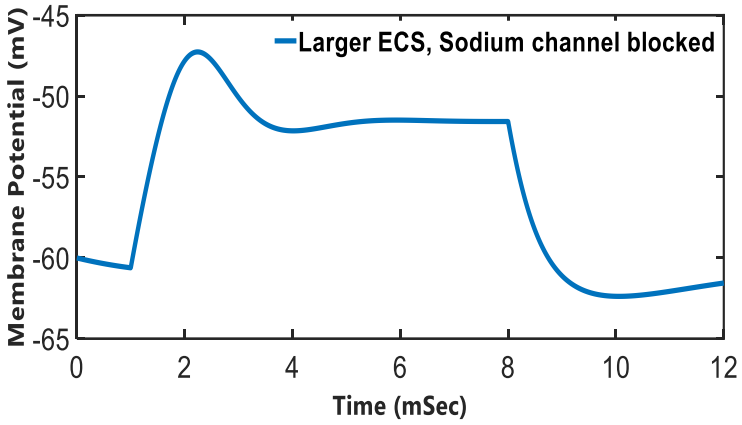

Fig.5.7 Spike Train when sodium channels are blocked, ECS = 100 nm

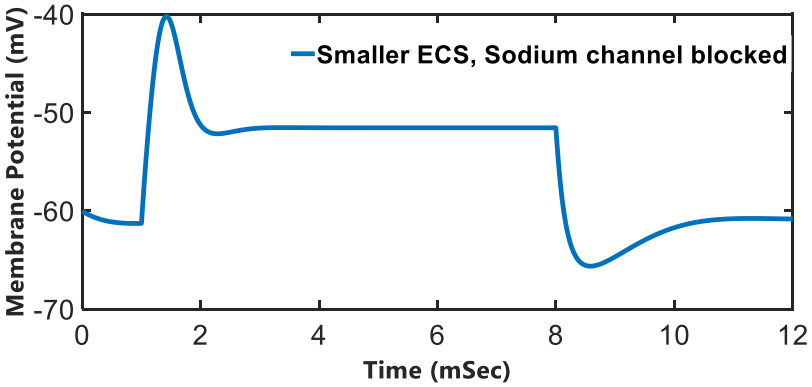

Fig.5.8 Spike Train when sodium channels are blocked, ECS=10 nm

In this section, it is assumed that any injury to the nerve fiber results in blocking of the sodium ion channels, leaving the potassium ion channels functional. Here, the blocking condition is applied to the maximal conductance of sodium ions i.e. g_{Na} in the H-H parameters which is kept at 0.01 which is almost negligible. This indicates that, only a limited number of sodium ion channels are kept open to generate an action potential, the figure for the above condition is shown in Fig.5.6. Here, the internal diameter of the fiber is kept at 5 μm and the size of the ECS is varied for each plot. Fig.5.6 shows the plot for sodium blocking condition with the size of the ECS kept at 50 nm, observing Fig.5.6, it is seen that the initial action potential is having a reduced amplitude (-43.5 mV) and the subsequent spikes as seen from Fig.5.3 are absent suggesting hypoexcitation. This occurs because the generation of an action potential depends on sodium ions; blocking these ion channels prevents sodium ions from entering the cell, changing the action potential's shape and form. Here, sodium channel blockage raises the threshold for the initiation of an action potential. The amplitude of the action potential is reduced, but it is still possible to cross this higher threshold if the depolarizing stimulation is strong enough. However, the signal would not be sufficiently strengthened and would experience a sharp decrease in amplitude due to the lack of sufficient sodium ion channels. Furthermore, Fig. 5.6 also shows that the resting membrane potential has a DC shift and that the signal undergoes a prolonged refractory period. This might occur because when sodium ion channels are blocked, there are insufficient sodium channels available to initiate another action potential, which inhibits the production of the other spikes thus prolonging the duration of refractory period over the same time frame. A reduction in sodium conductance can lead to a prolonged refractory period because voltage-gated sodium channels take longer to reopen after being inactivated. Since, the rapid depolarization of the membrane during an action potential is regulated by the voltage-gated sodium channels; a reduction in sodium conductance may cause a DC shift in the membrane potential. These symptoms of hypoexcitation are typically associated with conditions like sodium Channelopathies [203], [204], [205] and that of Guillain-Barré Syndrome [201], [202].

Under similar blocking condition, when the ECS is considered to be larger (100 nm) as seen from Fig.5.7, it can be said that the amplitude of the spike further diminishes to -47.4 mV which suggests that the effect of the ECS is evident in this scenario. Similar to the observations made from Fig.5.6, the resting membrane potential also undergoes a DC shift due to the reasons discussed above. The occurrence of prolonged refractory period is also observed from Fig.5.7 which suggests that the subsequent spikes of the spike train cease to occur causing

hypoexcitation like condition which are synonymous with diseases or conditions like Sodium Channelopathies and Guillain-Barré Syndrome. Meanwhile, if the size of the ECS is considered to be smaller (10 nm) as seen in Fig.5.8, the amplitude of the spike marginally increases and the occurrences of DC shift to the resting membrane potential and prolonged refractory period is also observed similar to Fig.5.6 and Fig.5.7. This result suggests that the ECS have a prominent role to play in governing neuronal signal generation and transmission through the combined effect of the sodium channel blocking and the size of the ECS.

B.2. Spike train when sodium ion conductance (intracellular sodium ion concentration) is increased

This section pertains to the assumption that any injury to the nerve fiber causes increase in the opening of the sodium ion channels leading to increased sodium concentration in the intracellular media. To represent the increased sodium ion condition, the maximal conductance of sodium ions i.e. g_{Na} in the H-H parameters is increased by a factor of 2. Moreover, the size of the ECS is considered to be of 50 nm and the internal diameter of the fiber is considered to be 5 µm.

It is seen from Fig.5.9 that the plot is similar to the one seen for a healthy nerve fiber which is shown in Fig.5.3 suggesting that a substantial increase to the intracellular sodium ion concentration does not change the shape and form of the nerve signal significantly. Because of the fundamental properties for the generation of the action potential, an increase in the number

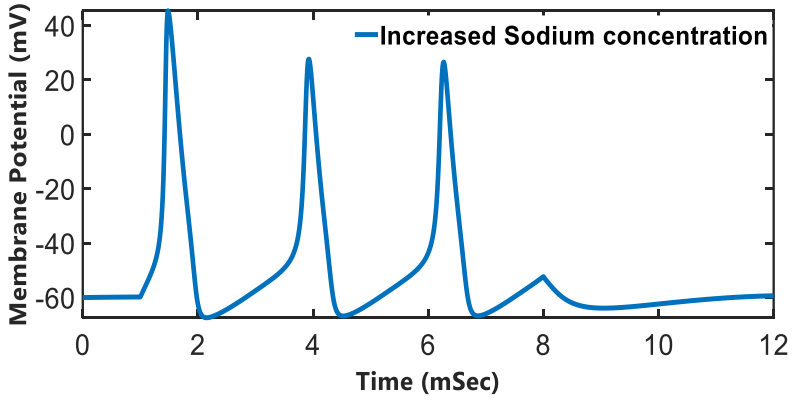

Fig.5.9 Spike Train when sodium ion concentration is increased due to injury, ECS = 50 nm

of open sodium ion channels does not always result in a substantial change in the action potential spike train. The initiation of action potential mainly depends on achieving the threshold voltage, a further increase in sodium conductance beyond the thresholds necessarily

does not contribute significantly to alter the shape and form of the action potential spike train because the concentration gradient of sodium influx has already been established.

B.3. Spike train when potassium ion channels are blocked

In this section, it is assumed that any injury to the nerve fiber resulted in blocking of the potassium ion channels, leaving the sodium ion channels functional. Here, the internal diameter of the fiber is kept at 5 µm and the size of the ECS is varied for each plot and the blocking condition is applied to the maximal conductance of potassium ions i.e. g_k in the H-H parameters which is kept at 0 indicating that the potassium ion channels are blocked.

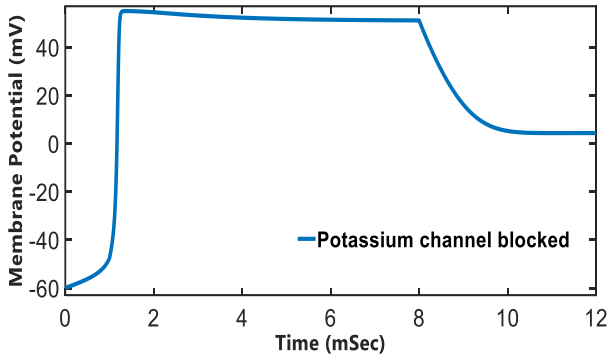

Fig.5.10 Spike Train when potassium channels are blocked, ECS= 50nm

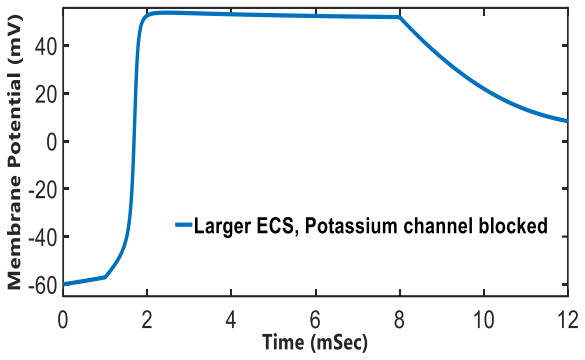

Fig.5.11 Spike Train when potassium channels are blocked, ECS =100 nm

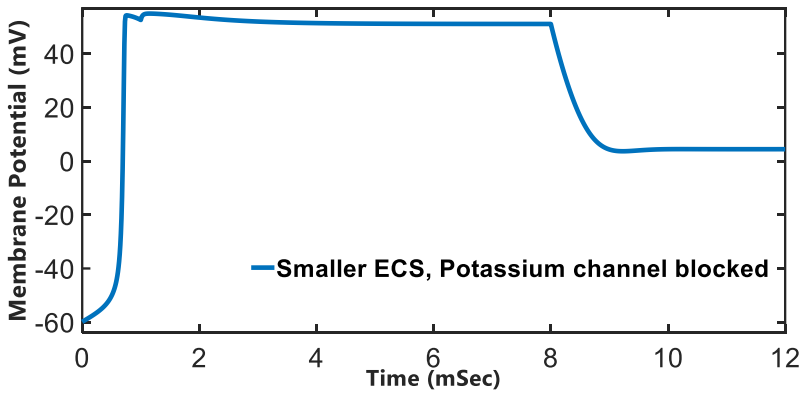

Fig.5.12 Spike Train when potassium channels are blocked, ECS = 10 nm

Initially the size of the ECS is considered to be of 50 nm and the resultant plot is shown in Fig.5.10. When compared to the blocking events of the sodium ion channel, it can be seen from Fig.5.10 that the action potential's amplitude here is greater i.e., about 55.1 mV. The action potential gets generated and is readily sustained because the sodium ion channels, which are essential for its formation are not blocked. However, because there are insufficient potassium ion channels which are essential to initiate the repolarization phase, the depolarization phase

of the action potential gets sustained for a longer duration. Since potassium ion channels play a crucial role in controlling the repolarization phase and refractory periods of excitable cells, blocking them results in the initial spike lasting the entire duration of the spike train suggesting hypoexcitation of the neuronal signal. This insufficient opening of the potassium ion channels offers hindrance to repolarize the initial spike, which prevents the subsequent spikes from being generated. This is demonstrated in Fig. 5.10, where the initial spike is sustained for the entire duration of the spike train. Furthermore, Fig. 5.10 also shows a rise in the signal's amplitude, or intensity. This is because blocking of the potassium channels can result in a prolonged depolarization phase by obstructing the neuron's capacity to repolarize efficiently. As a result, the action potential can amplify more, producing a stronger signal. Eventually, this scenario can be attributed to diseases associated with potassium channelopathies[206], [207], [208].

Now the simulation is carried out under similar potassium blocking conditions but the size of the ECS is considered to be larger i.e. the diameter of the ECS is considered to be of 100 nm, the internal diameter of the fiber is kept at 5 μm and the resultant plot obtained is shown in Fig.5.11. Although the action potential is generated efficiently in this instance, its amplitude somewhat lowers to 53.7 mV, which is because the ECS is assumed to be larger in this instance. Furthermore, as shown in Fig.5.10, there is a delayed repolarization, indicating a prolonged depolarization phase of the action potential and also the subsequent spikes failed to get generated suggesting hypoexcitation of the neuronal signal for the reasons previously mentioned. Diseases linked to potassium channelopathies may be associated to this condition [206], [207], [208].

Now, the simulation is carried out under similar blocking conditions, considering the size of the ECS to be smaller i.e. of 10 nm, with internal diameter of the fiber kept at 5 μm and the resultant plot is shown in Fig.5.12. It is observed from Fig.5.12, that the initial action potential spike gets generated and sustained effectively, but due to the smaller ECS causing hindrance to the outward movement of the ions from within the nerve fiber, the amplitude of the signal increased to about 55 mV. Moreover, similar to the one observed from Fig.5.10 and Fig.5.11, there is also an occurrence of delayed repolarization, indicating a prolonged depolarization resulting in hypoexcitation of the neuronal signal for the reasons mentioned above. These conditions can be attributed to conditions associated with potassium channelopathies [206], [208], [209].

B.4. Spike train when potassium ion conductance is increased

In this section, it is assumed that any injury to the nerve fiber results in an increased opening of the potassium ion channels causing increased efflux of potassium ions towards the extracellular media. The increased potassium condition is applied to the maximum conductance of potassium ions i.e. g_k in the H-H parameters which is increased by a factor of 2.

A balance of ion concentrations, with high level of potassium ion concentrations inside the cell and higher levels of sodium ion concentration outside the cell, maintains the normal resting potential. An electrochemical potential produced by this concentration gradient aids in the control of neuronal excitability. The disruption in the equilibrium of ion concentrations caused by an increased potassium ion conductance that may lead to increased efflux of potassium ions from the nerve fiber can result in quick repolarization of the cell membrane and due to the potassium ion channels kept normal, this rapid efflux of potassium ions results in quick repolarization of the cell membrane causing additional spikes to get generated within the same time frame thus suggesting hyperexcitation as seen in Fig.5.13. Fig.5.13 is generated considering the size of the ECS is considered to be if 50 nm and the internal diameter of the fiber is kept at 5 μm respectively. Moreover observing Fig.5.13, it is evident that the strength or magnitude of the signal does not change significantly as the size of the ECS is considered to be normal (50 nm). Here, the hyperexcitability brought on by an increase in extracellular potassium levels can have a variety of effects on neuronal functions such as spontaneous activation of action potentials, increased sensitivity to stimuli, and abnormal signalling patterns. These alterations may contribute to conditions such as epilepsy, in which the brain experiences recurrent and uncontrolled bouts of excessive neuronal activity, Peripheral Neuropathy, and Restless Legs Syndrome [195], [196], [197].

Now, the simulation is carried out under same condition of increased potassium conductance, but the size of the ECS is considered to be larger i.e. of 100 nm and the internal diameter of the fiber kept at 5 μm, the resultant plot is shown in Fig.5.14. It is seen from Fig.5.14 that when the size of the ECS is larger, the amplitude of the spike train drops and also the additional spike which is seen from Fig.5.13 is absent. This suggests that a larger ECS has a significantly higher impact on the neuronal signal or the action potential spike train as there is a greater leakage of ions from within the nerve fiber towards the external media which resulted in further attenuation of the neuronal signal. Here, signal modulation may not occur, meaning that the information may remain intact, but there is a possibility of information loss

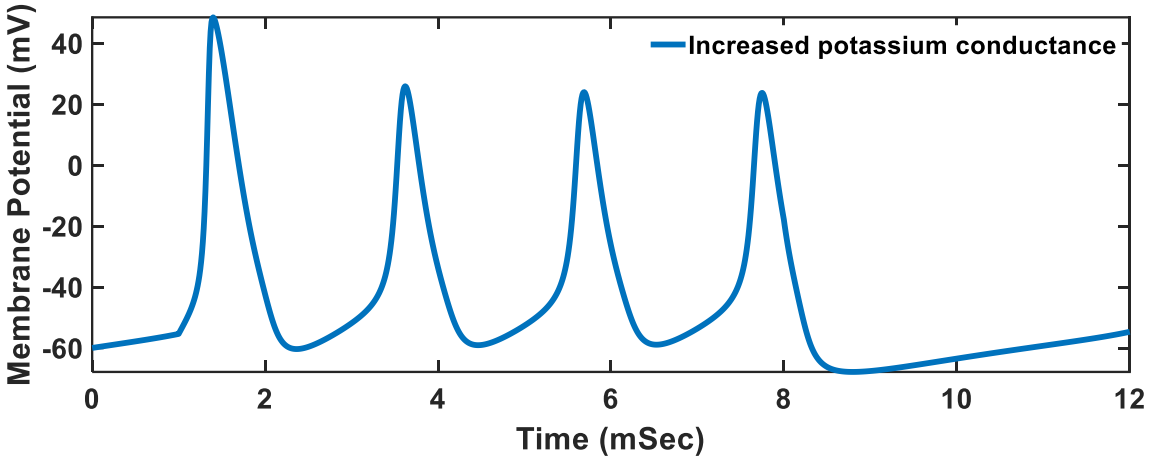

Fig.5.13 Spike Train when potassium conductance is increased, ECS = 50 nm

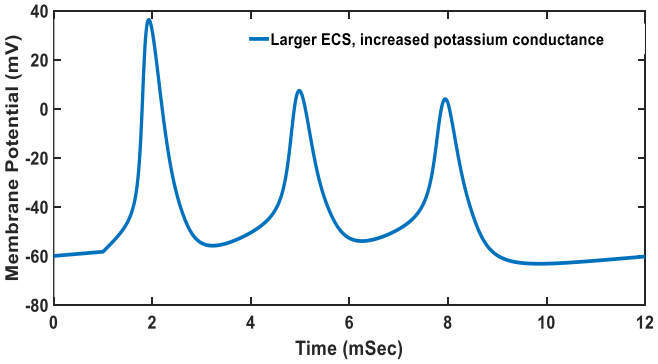

Fig.5.14 Spike Train when potassium conductance is increased, ECS= 100 nm

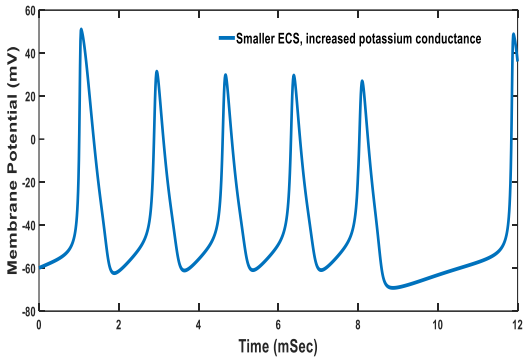

Fig.5.15 Spike Train when potassium conductance is increased, ECS = 10 nm

as the signal travels down the fiber due to the decrease in the signal amplitude. This decrease in signal strength is a typical indication of problems like peripheral neuropathy, Guillain-Barré syndrome, Charcot-Marie-Tooth condition etc.

Now the simulation is carried under same condition of increased potassium conductance, but the size of the ECS is considered to be smaller i.e. of 10 nm and with the internal diameter of the fiber kept at 5 μm, the resultant plot is shown in Fig.5.15. Fig.5.15 shows that for a smaller ECS, the number of spikes has increased significantly as compared to Fig.5.13 and Fig.5.14 and the amplitude of the signal has also increased. This is because the effect of the smaller ECS combined with the condition of increased potassium channels have aided in bring in massive hyperexcitation to the neuronal signal by fastening the process of repolarization within the same time frame and also proving hindrance to the leakage of ions towards the external media due to a smaller ECS. This kind of condition is synonymous with

neurological issues like severe epilepsy, Peripheral Neuropathy, Restless Legs Syndrome [195], [196], [197]. The summary of the observations made from the above is shown in Table.5.1.

To highlight the influence of similar ECS conditions, the following correlations are established between healthy and diseased nerve fibers. When the size of the ECS is 50 nm and the nerve fiber is healthy, the amplitude of the initial spike of the spike train is found to be 42.34 mV and the subsequent spike amplitude are found to be 20.02 and 18.37 respectively. For a similar sized ECS i.e. 50 nm and with sodium ion channels being blocked, the amplitude of the initial spike is found to be very small which is about -43.5 mV. Moreover, the subsequent spikes cease to exist which represents hypoexcitation of neuronal signal. Additionally, the resting membrane potential is found to undergo a DC shift and there is an occurrence of prolonged refractory period. This is because blocking sodium ion channels raises the threshold for action potential initiation which eventually cause a single spike to get generated with much difficulty but with low amplitude. Now, for an ECS of 50 nm and with sodium ion concentration being increased, it is seen that the spike train is similar to that of a healthy spike train when ECS is of the same size. This is because as the threshold for action potential initiation is already achieved, a further increase in sodium ion concentration in the intracellular fluid does not affect the shape and form of the spike train much. For an ECS of 50 nm and with potassium channels being blocked, it is observed that the amplitude of the initial spike is about 55.1 mV. The action potential gets generated and sustained for a longer duration of time. Prolonged depolarization is also observed since there is a lack of potassium ions needed for repolarization of the cell membrane and also there is an occurrence of hypoexcitation of the nerve signal due to the reason mentioned above. Now, for an ECS of 50 nm and with increased potassium conductance, it is observed that there is an occurrence of rapid repolarization of the nerve membrane resulting in hyperexcitation of the cell membrane, but the amplitude of the signal does not change significantly.

When the size of the ECS is larger i.e. 100 nm and the nerve fiber is healthy, it is seen that the amplitude of the initial spike of the spike train is about 23.75 mV, but the subsequent spikes of the spike train have reduced amplitude. It is also seen that there is a reduction in the number of spikes in the spike train suggesting hypoexcitation of the neuronal signal. For an ECS of 100 nm and with sodium ion channels being blocked, it is observed that the amplitude of the initial spike of the spike train reduces to about -47.4 mV. The resting membrane potential undergoes DC shift and also there is an occurrence of prolonged refractory period. Moreover, the subsequent spikes in the spike train also cease to exist which suggests hypoexcitation of

the neuronal signal. For an ECS of 100 nm and with potassium channels being blocked, it is observed that the amplitude of the initial spike of the spike train is about 53.7 mV, but there is an occurrence of delayed repolarization of the nerve fiber which suggests the occurrence of prolonged depolarization phase of the action potential spike train. The subsequent spikes in the spike train also fails to get generated suggesting hypoexcitation of the neuronal signal. For an ECS of 100 nm and potassium conductance being increased, it is observed that the amplitude of the initial spike of the spike train drops, and the additional spikes also fails to get generated which suggests a condition of hypoexcitation.

When the size of the ECS is smaller i.e. 10 nm and the nerve fiber is healthy, it is seen that the amplitude of the initial spike of the spike train is about 47.69 mV, and the amplitude of the subsequent spikes are also found to be increased. Furthermore, additional spikes are also found to be generated suggesting hyperexcitation of the neuronal signal. This occurs because of the ECS being smaller which aids in a better signal transmission. For an ECS of 10 nm and with sodium ion channels being blocked, it is observed that the amplitude of the spike train marginally increases and there is an occurrence of a DC shift to the neuronal signal and, prolonged refractory period is also observed under this condition. For a similar ECS i.e. 10 nm and with potassium ion channels being blocked, it is seen that the initial spike of the spike train gets generated and sustained effectively. The amplitude of the spike train is found to be increased to about 55 mV. There is also an occurrence of delayed repolarization suggesting prolonged depolarization of the nerve signal and also hypoexcitation of the neuronal signal is also observed. These observations are so made because of the combined effect of a smaller ECS and blocked potassium ion channels as potassium ions are necessary to bring the repolarization phase of the action potential. Again, for a similar sized ECS i.e. 10 nm and with potassium ion conductance being increased, it is observed that the number of spikes of the spike train has increased significantly. The amplitude of the spike train have also found to be increased and there is also an occurrence of hyperexcitation of the neuronal signal due to the faster repolarization phase initiated by increased potassium ion channels.

The ECS is essential for the distribution of chemotherapeutic drugs therefore, the proposed framework, with its simple membrane potential expression given in Eq.5.13, may prove useful regard. It might also help in the diagnosis, prediction, and understanding of different neurological conditions impacted by ECS of different sizes. The simulation results generated through Eq.5.13 seem to be in line with previous research and might be essential to understanding how the ECS influences neuronal signals.

Table 5.1: Summary of the observations made from section 5.5.1

Size of the ECS	Fiber status	Ionic condition	Signal Strength	Signal condition	Symptoms of possible Medical conditions
Smaller	Healthy	Normal	Increased	Hyperexcitation	Epilepsy, Peripheral Neuropathy, Restless Legs Syndrome
Larger	Healthy	Normal	Decreased	Hypoexcitation	Guillain-Barré Syndrome, Charcot-Marie-Tooth Condition
Normal	Injured	Sodium channels blocked; Potassium channels normal	Decreased	Prolonged refractory period; dc shift to membrane potential; Hypoexcitation	Sodium Channelopathies, Guillain-Barré Syndrome
Larger	Injured	Sodium channels blocked; Potassium channels normal	More decreased	Prolonged refractory period; dc shift to membrane potential; Hypoexcitation	Sodium Channelopathies, Guillain-Barré Syndrome
Smaller	Injured	Sodium channels blocked; Potassium channels normal	Marginal increased	Prolonged refractory period; dc shift to membrane potential; Hypoexcitation	Sodium Channelopathies, Guillain-Barré Syndrome
Normal	Injured	Increased Sodium conductance; Normal Potassium conductance	No significant change	Similar to normal spike train	-
Normal	Injured	Potassium channels blocked; Sodium channels normal	Increased	Delayed repolarization; Prolonged depolarization; Hypoexcitation	Potassium Channelopathies
Larger	Injured	Potassium channels blocked; Sodium channels normal	Marginal decreased	Delayed repolarization; Prolonged depolarization; Hypoexcitation	Potassium Channelopathies
Smaller	Injured	Potassium channels blocked; Sodium channels normal	Marginal increased	Delayed repolarization; Prolonged depolarization; Hypoexcitation	Potassium Channelopathies
Normal	Injured	Increased Potassium conductance; Normal Sodium conductance	No significant change	Hyperexcitation	Epilepsy, Peripheral Neuropathy, Restless Legs Syndrome
Larger	Injured	Increased Potassium conductance; Normal Sodium conductance	Decreased	Similar to normal spike train	-
Smaller	Injured	Increased Potassium conductance; Normal Sodium conductance	Increased	Severe Hyperexcitation	Epilepsy, Peripheral Neuropathy, Restless Legs Syndrome

The framework is particularly effective to obtain an approximate result which could also be used for rapid prototyping and has a reduced computing complexity. It has already been established that the ECS plays a critical role in regulating the generation and propagation of action potential, thus incorporation of the fundamental parameters of the ECS into the

final membrane potential expression as shown in Eq.5.13, allows for a detailed study of neuronal signal transmission.

5.5.2 Genetic Mutation of ion channels and application of Rescue protein mechanism to alter its effects

Genetic mutations can cause a shift in the voltage dependence of gating variables (m, n, and h) through changing its rate constants (α and β) which leads to the ion channels opening or closing at inappropriate voltage threshold, examples of these genes are those encoding potassium (KCNA and KCNQ genes) and sodium (SCN genes). In this section, the work involves incorporation of the rescue protein mechanism given in Eq.5.14 to alter the effect of genetic mutation of ion channels and to restore the normal propagation of the neuronal signal. Here, the rescue protein mechanism is applied considering two scenarios; one in which there is a positive voltage shift to the rate constant parameters, and the other in which there is a negative voltage shift to the rate constant parameters. This voltage shift is intended to simulate the possible effects of genetic mutation on the voltage-dependent activation and inactivation properties of the ion channels which shows a scenario where the channel gates open or close at more positive or more negative membrane potentials. For the simulation purpose, the size of the ECS is kept fixed at 50 nm and the internal diameter of the fiber is kept fixed at 5 μm.

5.5.2.1 Implementation of Rescue protein mechanism

The rescue protein mechanism has been incorporated into the proposed framework as rescue protein voltage $R_p(V_m)$ which is assumed to be a combination of the original and the mutated membrane potential which can be shown as,

$$R_p(V_m) = (1 - k_{Rescue})V_{m,Original} + k_{Rescue}V_{m,mutated} \quad (5.14)$$

Here, k_{Rescue} is the rescue (protein) coefficient serves as a tuning parameter that regulates how much a rescue protein mechanism counteracts the effects of a mutation. The parameter allows for fine-grained control over the degree of rescue by seamlessly transitioning between the mutated state and the non-mutated state. $V_{m,original}$ and $V_{m,mutated}$ represents the membrane potential for the non-mutated (original) scenario and for the mutated scenario respectively. $(1\text{-}k_{Rescue})$ denotes the contribution of the non-mutated scenario to the resulting membrane potential which may be regarded as the proportion of the original membrane potential that remains unaltered due to mutation. When k_{Rescue} is 0, then $(1\text{-}k_{Rescue})$ becomes 1, which signifies that the rescue protein mechanism has successfully restores the system back to

its non-mutated (original) scenario. As k_{Rescue} increases gradually, $(1-k_{Rescue})$ starts decreasing thereby reducing the effect of the original trace. This suggests that the rescue effect is also decreasing, and the membrane potential is more influenced by the mutated condition. This formula is used to interpolate between the original and mutated membrane potential traces allowing the model to simulate various proportion of rescue operations. Studying the impact of partial or full rescue mechanisms in response to genetic mutations is made easier by manipulating k_{Rescue}, which controls the extent to which the rescue protein restores functional nerve function. In this work, the rescue protein mechanism is applied through the implementation of Eq.5.14 and the simulation is run for rescue coefficient $(k_{Rescue}) = 1$ and for rescue coefficient $(k_{Rescue}) = 0$.

When $k_{Rescue} = 1$, then according to Eq.5.14, the rescue protein voltage $R_p(V_m)$ becomes exactly same as the mutated voltage $(V_{m,mutated})$ suggesting that there is no rescue taking place. Here, the rescue protein does not change the mutated membrane potential meaning that the rescue mechanism has failed, and the mutation still has a complete effect on the neuron dynamics. Additionally, gating variables remain in their mutated form further indicating that the mutation has completely overtaken the system's behaviour.

When $k_{Rescue} = 0$, then according to Eq.5.14, the rescue protein voltage $R_p(V_m)$ becomes exactly same as the non-mutated (original) voltage i.e., $V_{m,mutated}$. In this scenario, the dynamics of the membrane potential revert to their non-mutated (normal) condition and the dynamics of the gating variables (m, n, and h) also revert to normal as though mutation had never occurred. Thus, full rescue occurs when on the application of the rescue protein voltage $R_p(V_m)$, the rescue curve merges with that of the original plot suggesting that the original membrane potential has been regained and the effect of mutation nullified. Thus, the rescue coefficient (k_{Rescue}) should lie between 0 and 1 depending upon the degree of rescue taking place where $k_{Rescue} = 1$ suggesting no rescue and $k_{Rescue} = 0$ suggesting complete rescue. The adjustment in the value of k_{Rescue} enables precise control over the degree to which the rescue protein corrects for the mutation. This rescue coefficient enables for a thorough investigation of the rescue protein mechanism and how the rescue mechanism might work under different circumstances. Because of its adaptability, k_{Rescue} is an essential tool for researching various possible consequences of rescue proteins and comprehending how well they work to restore normal nerve activity.

To induce the ion channel mutation, the rate constants (α, β) given in Eq.5.10 are updated according to the voltage change which would eventually update the gating variables (m, n, and h). Moreover, to implement the rescue protein mechanism, the rescue protein voltage has been introduced to the rate constants (α, β) given in Eq.5.10 which would again update the gating variables.

The gating variable (m, n, and h) are updated according to the rescue protein voltage $R_p(V_m)$ and these gating variables in-turn controls the ionic currents viz, sodium ion current, potassium ion current, and the leakage current. The updated gating variable after implementation of the rescue protein voltage can be shown as,

$$\frac{dn}{dt} = \propto_n (R_p(V_m))(1 - n) - \beta_n(R_p(V_m))n$$

$$\frac{dm}{dt} = \propto_m (R_p(V_m))(1 - m) - \beta_m(R_p(V_m))m$$

$$\frac{dh}{dt} = \propto_h (R_p(V_m))(1 - h) - \beta_h R_p(V_m)h \quad (5.15)$$

Similarly, the ionic currents also gets updated with respect to the rescue protein voltage $R_p(V_m)$ which can be shown as,

$$I_{Na} = G_{Na}\left(R_p(V_m) - E_{Na}\right) \quad (5.16)$$

$$I_k = G_k\left(R_p(V_m) - E_k\right) \quad (5.17)$$

$$I_l = G_l\left(R_p(V_m) - E_l\right) \quad (5.18)$$

C. Application of Rescue protein mechanism to alter the positive voltage shift to the Rate constant (α, β)

Initially, it is assumed that genetic mutation may result in a positive voltage shift to the rate constant parameters (α, β) and to reflect this voltage shift, a +10 mV shift to the voltage is duly applied to Eq.5.10 which would also update the gating variables (m, n, and h) and subsequently update the ionic currents; thus, Eq.5.13 is simulated using the above considerations to show the mutated scenario. Additionally, the rescue protein mechanism as shown in Eq.5.14 is

applied to check whether the effect of mutation is reversed or persist to exist through its application. The simulation is conducted within the time duration of 0-30 mSec window.

C.1 For Rescue coefficient (k_{Rescue})=1

In this section, the rescue protein mechanism is applied in the form of the rescue protein voltage $R_p(V_m)$, shown in Eq.5.14 for a mutated scenario which led to a positive voltage shift (+10 mV) to the rate constant parameters (α, β) and for rescue coefficient (k_{Rescue})=1. The original, mutated and rescue plots are shown in blue, red, and green colours respectively.

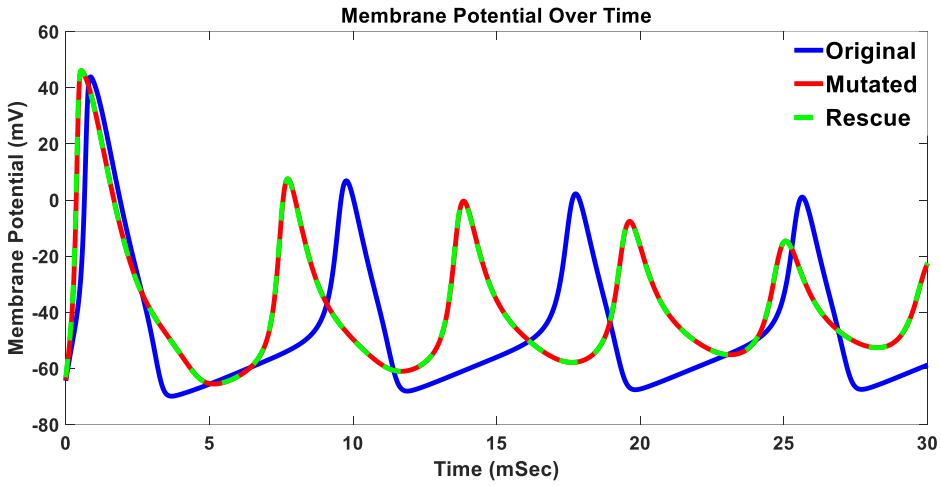

Fig.5.16 Non-mutated (original), mutated and Rescue (k_{Rescue}=1) membrane potential over time for +10 mV voltage shift in rate constant

The membrane potential plot over time for the original (non-mutated), mutated and rescue scenarios is displayed in Fig. 5.16. Observing the mutated plot, it can be seen that there is a rapid depolarization of the membrane potential in response to a +10 mV voltage shift to the rate constant which modifies the gating kinetics. This suggests that more spikes are generated, or hyperexcitation of the neuronal signal takes place within the same time frame. Also, the mutated spike train slightly shifts towards left in time axis showing faster response. Moreover, under a positive voltage shift, the initial spike tends to have a slightly higher amplitude, and the subsequent spikes of the mutated spike train decrease over time. When the rescue protein mechanism is incorporated into the model with rescue coefficient k_{Rescue}=1, then it is seen that the rescue mechanism fails as the rescue plot overlaps with the mutated plot (green and red plots) suggesting that the effect of genetic mutation is prevalent and overpowers

the effect of the rescue protein. Thus, the proposed mechanism could replicate the effect of a failed rescue where the effect of genetic mutation of ion channels still dominates neuronal excitation.

Fig.5.17 shows the plots for the gating variables (m, n, and h) for non-mutated (original), mutated and rescue scenarios. These gating variables represents the possibility of

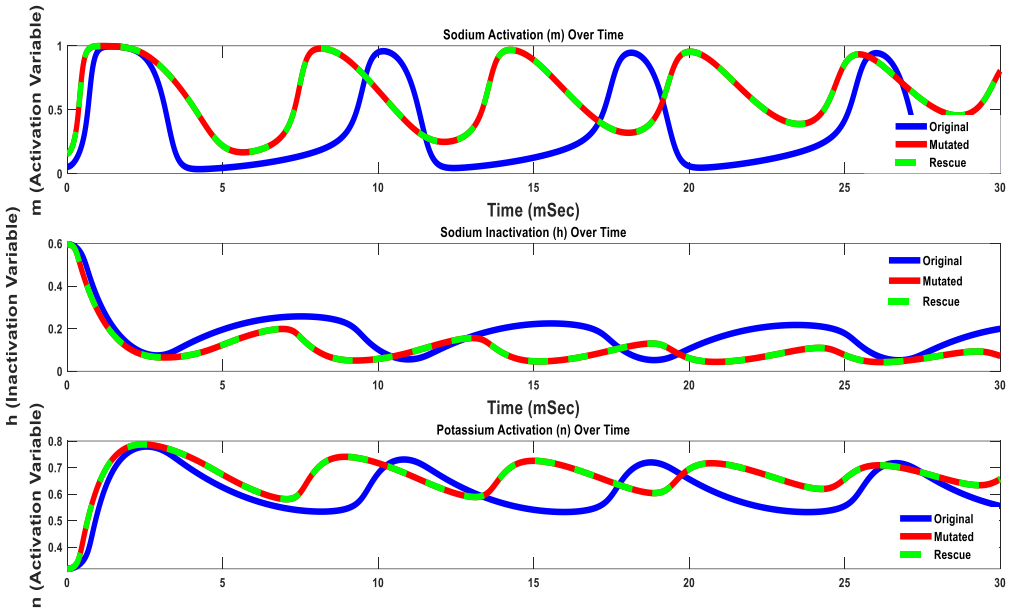

Fig.5.17 Non-mutated (original), mutated and Rescue (k_{Rescue}=1) gating variables over time for +10 mV voltage shift in rate constant

opening or closing of the ion channels and play a very vital role in exchanging ions viz, potassium (K^+) and sodium (Na^+) ions across the cell membrane during the duration of an action potential. The time courses of the gating variables (m, n, and h) changes when their voltage dependency varies by +10 mV as a result of mutation, as seen from the mutated plot in Fig. 5.17. When the sodium activation variable (m) variable rises to a higher level and activates more rapidly increasing the sodium current along the way, the sodium ion influx happens sooner and is more visible. This rapid activation of the sodium ion channels is one of the factors for causing hyperexcitation of the neuronal signal. The potassium activation variable (n) also activates more quickly in the mutated scenario due to the increased excitability and depolarization caused by the sodium channel mutation. This faster activation further aids in a larger and a quicker potassium current thereby aiding in a faster repolarization of the membrane potential following an action potential. Due to this quicker activation kinetics, the neuron might cross the threshold required for firing an action potential more quickly. This

causes the mutated spikes to shift to the left (faster in time) in the time axis, which increases the frequency of firing rate within the given time frame. Implementing the rescue protein mechanism given in Eq.5.14, with rescue coefficient k_{Rescue}=1, it is seen that the rescue mechanism fails as the rescue plot overlaps with the mutated plot (green and red plots) suggesting that the effect of genetic mutation still persists which also validates that the proposed mechanism could replicate the effect of failed rescue for gating variables and the effect of genetic mutation of ion channels dominates the neuronal excitation.

The effect of hyperexcitation is evident when looking at the mutated plots in Figs. 5.18(a), 5.18(b), and 5.18(c), which show the plots for sodium, potassium, and leakage current over time for the original, mutated and rescue scenarios respectively. These plots show an increase in the frequency of the sodium current, potassium current, and leakage current over time which is due to the faster activation of the gating dynamics corresponds to the observations made from Fig.5.17. This faster gating dynamics increases the overall ionic currents which contributes to an occurrence of hyperexcitation like scenario as seen from the mutated curve. On application of the rescue protein mechanism for rescue coefficient k_{Rescue}=1, it is seen that the effect of rescue protein mechanism fails, and the effect of mutation overtakes the rescue mechanism. This suggests that the proposed mechanism could replicate the effect of failed rescue for ionic currents in which the effect of genetic mutation of ion channels dominates neuronal excitation.

Fig.5.19 illustrates the phase plane plot of the sodium activation variable (m) against the membrane potential (V) for the non- mutated (original), mutated and the rescue scenarios for a positive voltage shift (+10 mV) to the rate constant parameters. The dynamics interaction between different components can be better understood through the phase plane plot. The occurrence of hyperexcitation and the faster response of the action potential spike train can be also correlated with the phase plane plot for a +10 mV voltage shift as seen in Fig.5.19. The

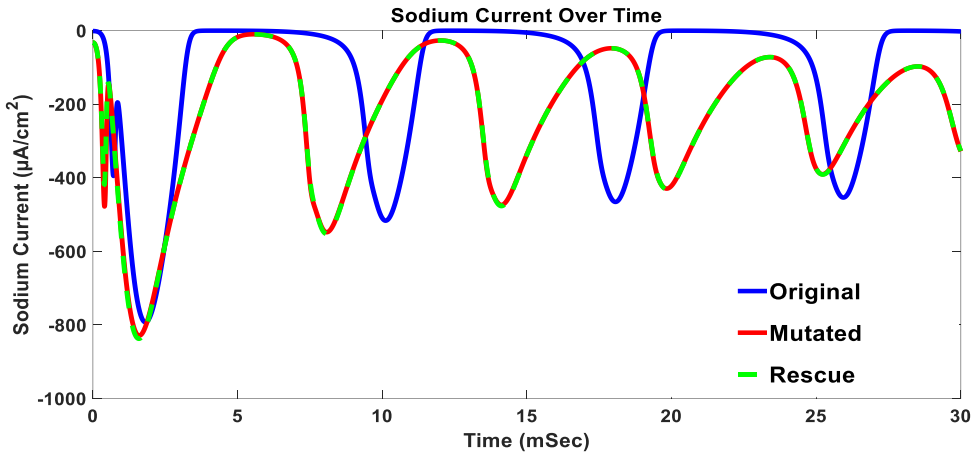

(a)

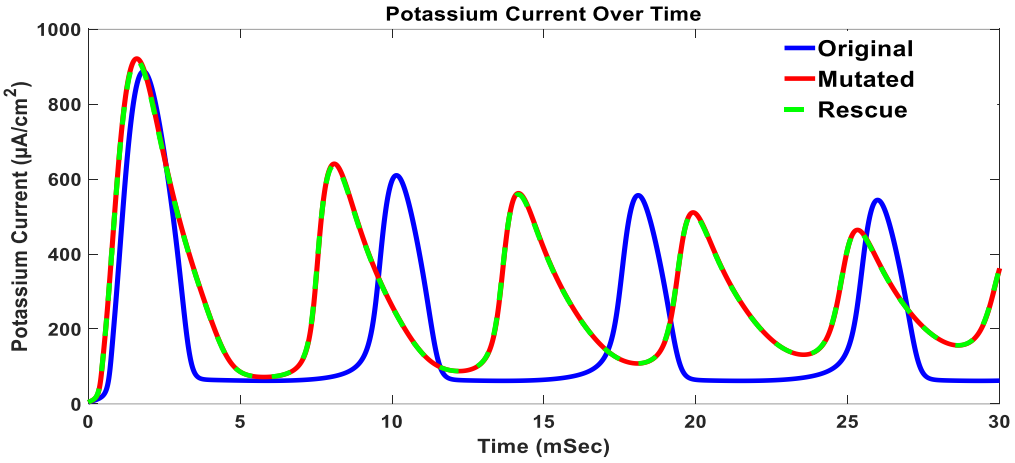

(b)

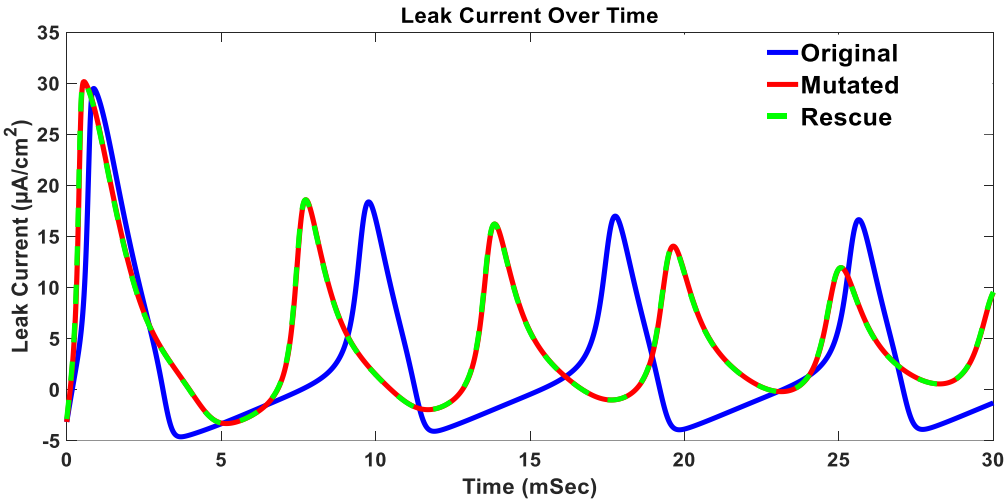

(c)

Fig.5.18 Variation in ionic currents for non-mutated (original), mutated and Rescue (k_{Rescue}=1) conditions over time for +10 mV voltage shift in rate constant (a). For Sodium current (b). For Potassium current (c). For Leakage current

phase plane plot in the non-mutated (original) scenario shows a typical loop, which illustrates

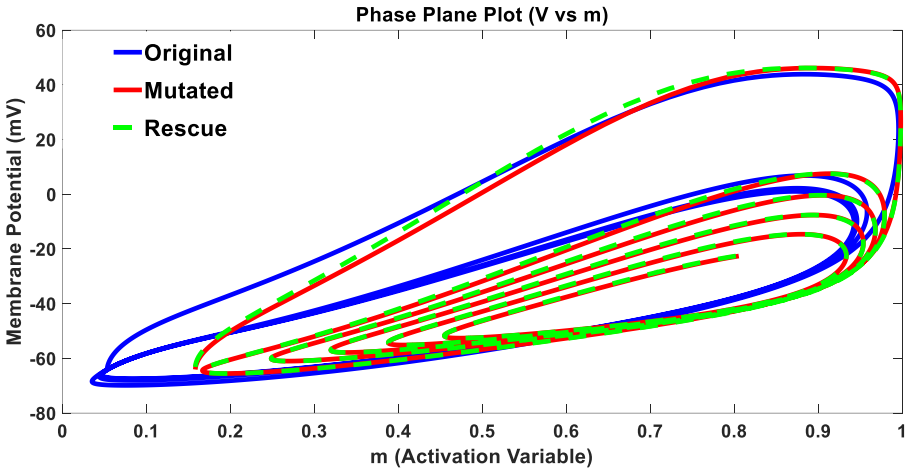

Fig.5.19 Phase plane plot (V vs m) for +10 mV voltage shift in rate constant for non-mutated (original), mutated and Rescue (k_{Rescue}=1) scenarios

the membrane potential of the neuron and the activation of sodium ion channels during an action potential. After the action potential reaches its peak, the plot shows a downward trajectory due to the opening of the potassium ion channels and closing of the sodium channels, thus showing the initiation of the repolarization phase. The loop eventually closes when the sodium activation variable and membrane potential return to their resting values, indicating the end of the action potential cycle. In the mutated scenario (+10 mV voltage shift), the phase plane plot clearly shifts indicating the enhanced excitability of the neuron as seen by a larger and more noticeable loop as both the sodium activation and the membrane potential rise more quickly at the beginning of the trajectory. Due to the greater sensitivity of the sodium channels for a +10 mV voltage shift, the neuron attains a higher membrane potential faster resulting in an increased depolarization. As a result, the membrane potential loop extends further along the axis and reaches a higher peak, indicating a larger sodium ion influx and the subsequent generation of multiple action potential spikes which is an indication of hyperexcitation like situation. The phase plane plot clearly demonstrates this aspect of genetic mutation by showing many loops or a more complex trajectory suggesting recurrent cycles of depolarization and repolarization. Moreover, when the rescue protein mechanism is applied for rescue coefficient k_{Rescue}=1, it can be seen again that the recue mechanism fails, and the mutation completely overtakes the neuronal excitation as the rescue plot overlaps with the mutated plot (green and red plots).

C.2 For Rescue coefficient (k_{Rescue})=0

In this section, the rescue protein mechanism is applied in the form of the rescue protein voltage $R_p(V_m)$, shown in Eq.5.14 for a mutated scenario which may lead to a positive voltage shift (+10 mV) to the rate constant parameters (α, β) and for rescue coefficient (k_{Rescue})=0. The original, mutated and rescue plots are shown in blue, red, and green colours respectively.

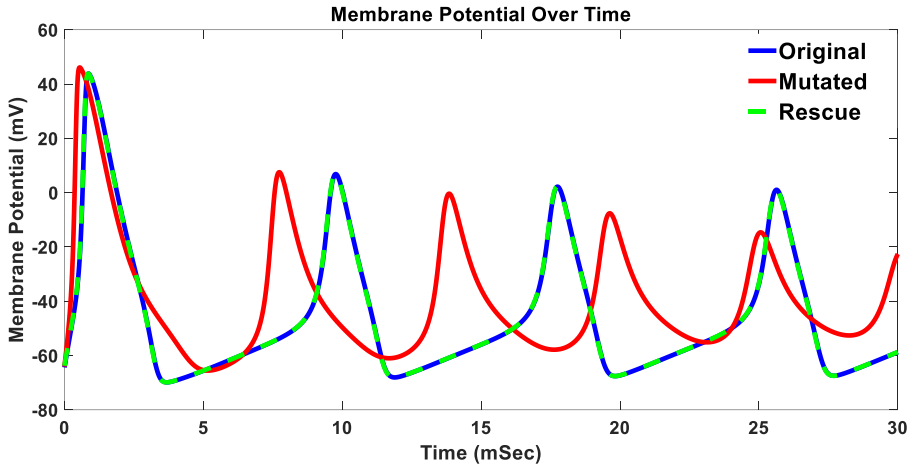

Fig.5.20 Non-mutated (original), mutated and Rescue (k_{Rescue}=0) membrane potential over time for +10 mV voltage shift in rate constant

The membrane potential plot over time for the original (non-mutated), mutated and rescue scenarios is displayed in Fig. 5.20. When the rescue coefficient (k_{Rescue})=0 is applied to the model, it can be seen that the effect of genetic mutation of ion channels gets completely nullified and the membrane potential returns to its initial non-mutated condition which is evident from Fig.5.20 as the rescue plot overlaps with the non-mutated (original) plot (green and blue plots). This suggest that the proposed mechanism could replicate the effect of complete rescue of the neuronal signal where the effect of genetic mutation of ion channels is mitigated, and the normal neuronal excitation is restored. This is also evident by observing the plots for the gating variables (m, n, and h) for non-mutated (original), mutated and rescue scenarios shown in Fig.5.21.

In Fig.5.21, it can also be seen that when the rescue coefficient (k_{Rescue}) is considered to be 0, the rescue plot completely overlaps with the original plot (green and blue plots)

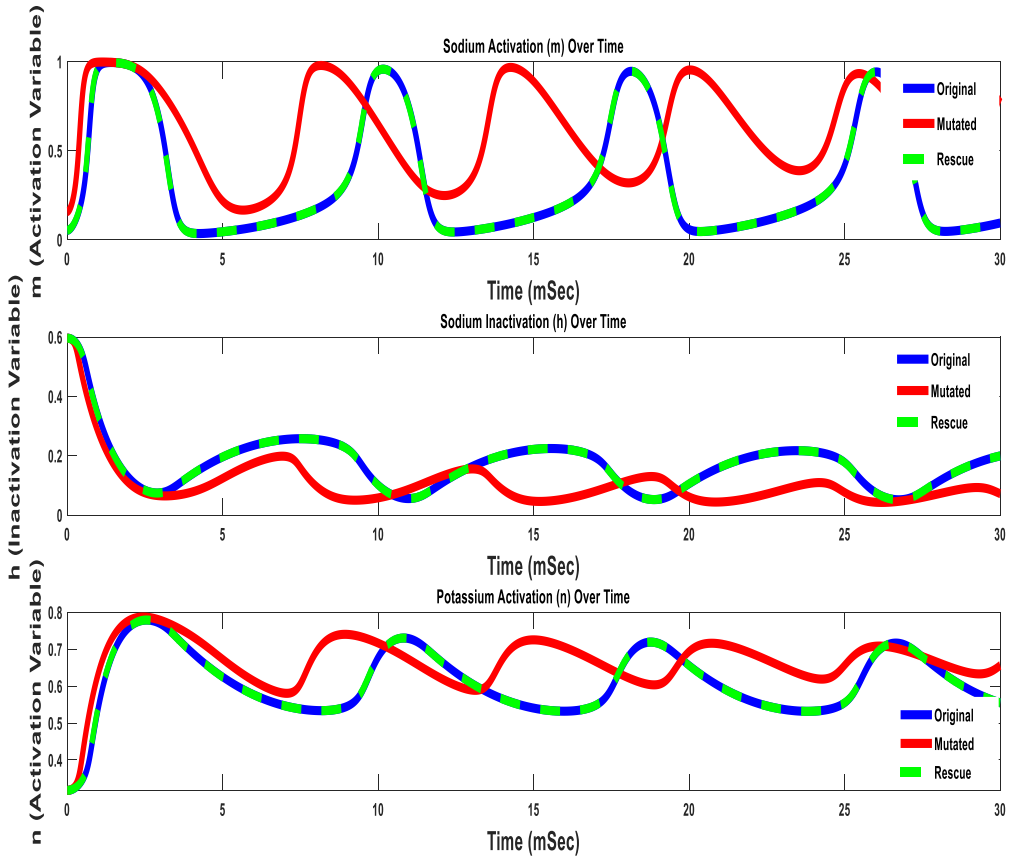

Fig.5.21 Non-mutated (original), mutated and Rescue (k_{Rescue}=0) gating variables over time for +10 mV voltage shift in rate constant

suggesting that the normal neuronal excitation is restored back. Thus, the proposed mechanism effectively manages to replicate the complete restoration of the neuronal excitation by mitigating the effect of genetic mutation of the ion channels as seen from the gating variable plots shown in Fig.5.21.

Figs 5.22(a), 5.22(b), and 5.22(c) shows the effect of application of the rescue protein mechanism with k_{Rescue} = 0, on the sodium, potassium and leakage current. It is also seen from Fig.5.22 that the rescue plot completely overlaps with the non-mutated (original) plots (green and blue plots) suggesting that the rescue mechanism effectively manages to mitigate the effect of genetic mutation on the ionic currents by restoring the ionic currents back to its original state. The phase plane plot shown in Fig.5.23 for rescue coefficient (k_{Rescue}) = 0 further substantiates the effective rescue mechanism for the mutated scenarios back to its original form and shape as the rescue plot completely merges with the original plot suggesting that the effect of mutation is nullified, and the normal neuronal excitation is restored effectively.

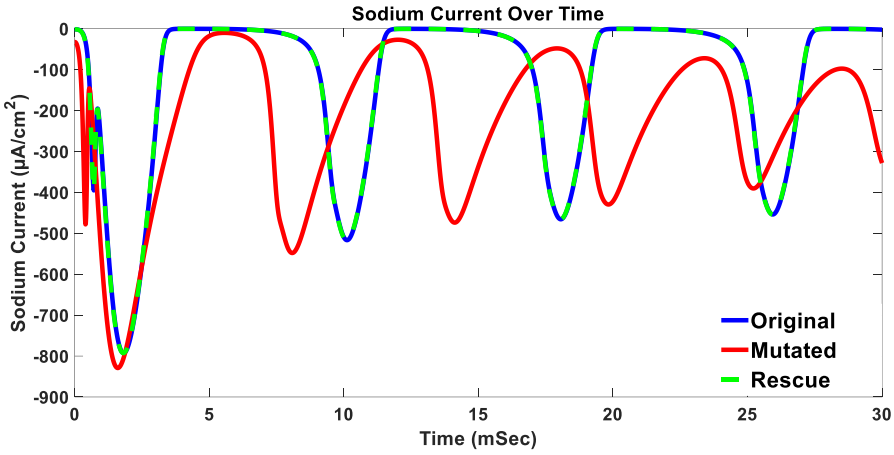

(a)

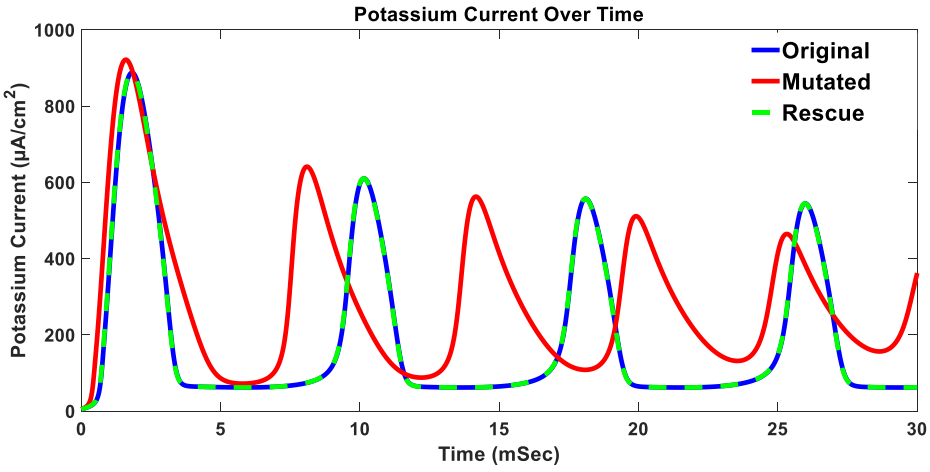

(b)

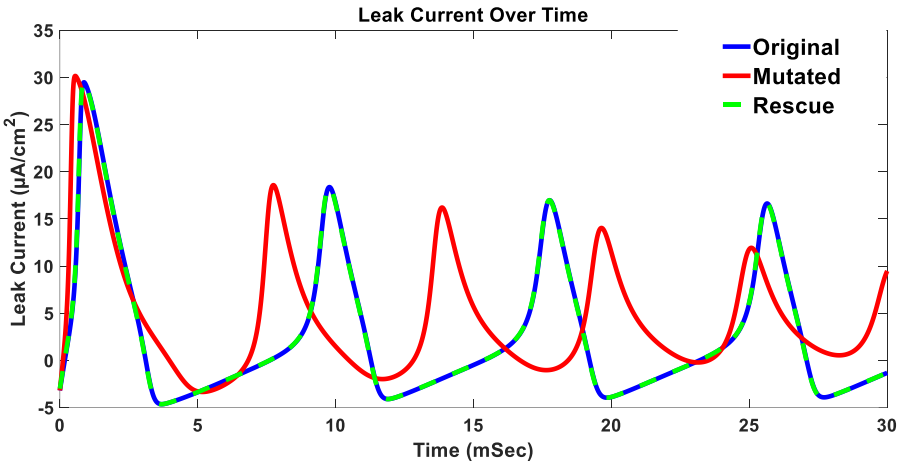

(c)

Fig.5.22 Variation in ionic currents for non-mutated (original), mutated and Rescue (k_{Rescue}=0) conditions over time for +10 mV voltage shift in rate constant (a). For Sodium current (b). For Potassium current (c). For Leakage current

Mutations in sodium channels, such as those in the SCN1A, SCN2A, or SCN8A genes, have

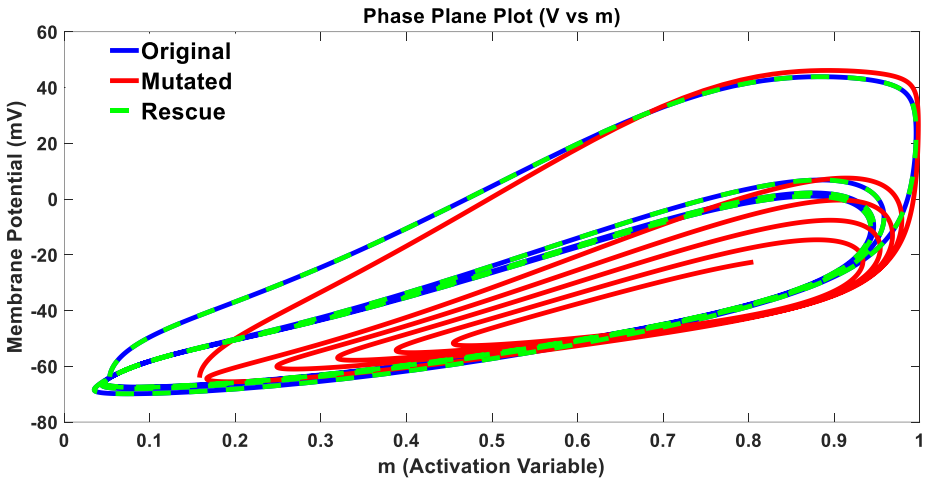

Fig.5.23 Phase plane plot (V vs m) for +10 mV voltage shift in rate constant for non-mutated (original), mutated and Rescue (k_{Rescue}=0) scenarios

been firmly linked to a range of neurological conditions, including epilepsy (hyperexcitation) [174], [176], [180] which results in channelopathies causing severe impact on neuronal excitation. For instance, mutations in the SCN1A gene are known to be associated with Dravet syndrome, a severe form of epilepsy marked by frequent, prolonged seizures that often start at infancy [181], [182]. Moreover, these mutations can lead to Genetic Epilepsy with Febrile Seizures Plus (GEFS+) [210], [211], a disease in which a person has febrile seizures along with a range of other neurological symptoms often starts with a feverlike symptom. Children with GEFS+ may continue to have seizures after they reach the typical age, but most children with uncomplicated febrile seizures outgrow them. Myoclonic seizures, focal epilepsy, generalized epilepsy, and other forms of epilepsy can all result from the disease. Apart from epilepsy, alterations in the sodium channel can result in a variety of disorders referred to as channelopathy-associated syndromes where the altered sodium channel gating causes aberrant neuronal excitability and abnormal action potential firing.

D. Application of Rescue protein mechanism to the negative voltage shift to the Rate constant (α, β)

Now, the simulation is undertaken assumed that genetic mutation may result in a negative voltage shift to the rate constant parameters (α, β) and to reflect this voltage shift, a -10 mV shift to the voltage is duly applied to Eq.5.10 which would also update the gating variables (m, n, and h) and subsequently update the ionic currents; thus, Eq.5.13 is simulated using the above considerations to show the mutated scenario. Additionally, the rescue protein mechanism as

shown in Eq.5.14 is applied to check whether the effect of mutation is reversed or persist to exist through its application. The simulation is conducted within the time duration of 0-30 mSec window.

D.1 For Rescue coefficient (k_{Rescue})=1

In this section, the rescue protein mechanism is applied in the form of the rescue protein voltage $R_p(V_m)$, shown in Eq.5.14 for a mutated scenario which led to a negative voltage shift (-10 mV) to the rate constant parameters (α, β) and for rescue coefficient (k_{Rescue})=1. The original, mutated and rescue plots are shown in blue, red, and green colours respectively.

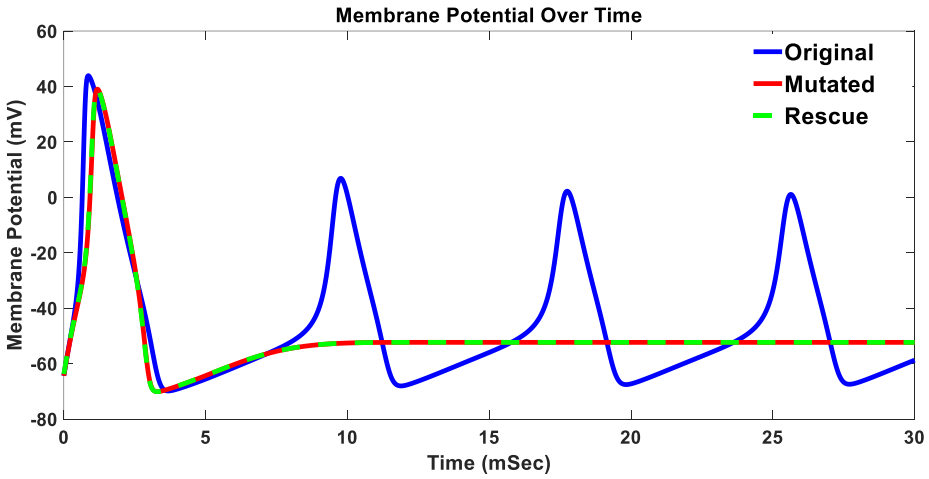

Fig.5.24 Non-mutated (original), mutated and Rescue (k_{Rescue}=1) membrane potential over time for -10 mV voltage shift in rate constant

The plot of membrane potential against time for non-mutated (original), mutated and rescue scenarios for a genetic mutation causing a negative voltage shift (-10 mV) is shown in Fig. 5.24. Observing Fig.5.24, it can be seen that the initial resting membrane potential, which is typically between -60 and -65 mV, is found to be same in both the non-mutant (original) and mutated scenarios which matches the typical resting potential of a neuron. However, the amplitude of the mutated curve decreases, and the action potential spike slightly shifts towards right in time axis suggesting delayed reaction. The subsequent spikes as seen from the non-mutated (original) plot of Fig.5.24 does not get generated in the mutated scenario suggesting hypoexcitation of the neuronal signal. In addition, a prolonged refractory period is also visible in the mutated case, where a single spike persists for the entire duration of the spike train, this shows how sensitive neural behaviour can become even for a small change in the gating dynamics. When the rescue protein mechanism is incorporated into the model for rescue

coefficient (k_{Rescue})=1, then it is seen that the rescue mechanism fails to counter the effect of mutation suggesting that the effect of genetic mutation is prevalent and overpowers the effect of the rescue protein which is evident from Fig.5.24 where the rescue plot overlaps with the mutated plot (green and red plots). Thus, the proposed mechanism could replicate the effect of a failed rescue where the effect of genetic mutation of ion channels still dominates neuronal excitation. This is further emphasised upon by the gating variables (m, n, and h) for non-mutated (original), mutated and rescue scenarios as shown in Fig.5.25.

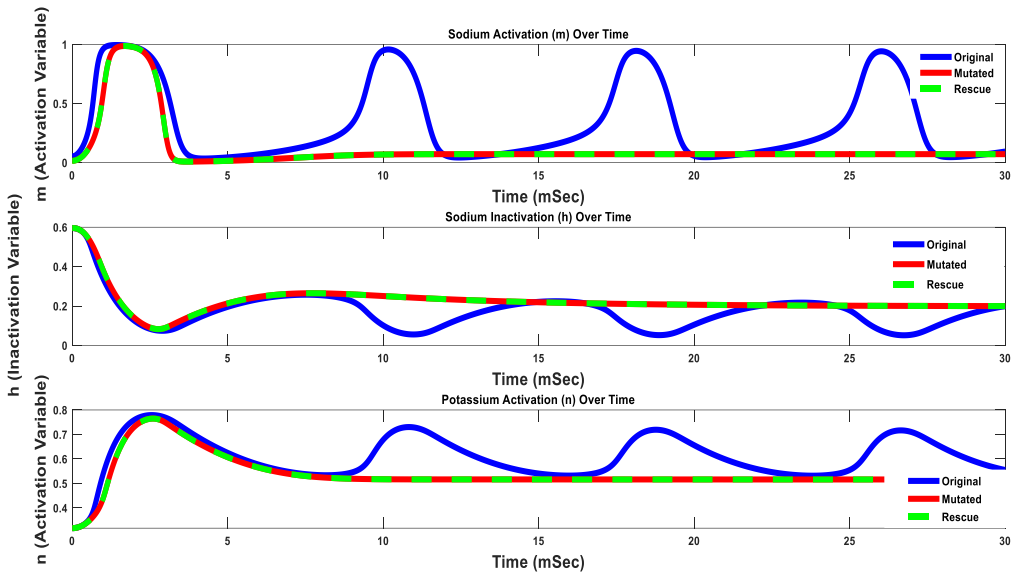

Fig.5.25 Non-mutated (original), mutated and Rescue (k_{Rescue}=1) gating variables over time for -10 mV voltage shift in rate constant

These gating variables represents the possibility of opening or closing of the ion channels and play a very vital role in exchanging ions viz, potassium (K^+) and sodium (Na^+) ions across the cell membrane during the duration of an action potential. Fig.5.25 shows that the neuron becomes less excitable and produces weaker, delayed action potentials, which contributes to the occurrence of hypoexcitation like possibilities which is brought on by a disruption in the gating dynamics that prevents the channels from recovering to a state where more action potentials can be produced after the initial spike causing a greater impact on how neurons respond to stimuli and transmit signals. Due to the negative voltage shift, the sodium ion channels have trouble activating resulting in a reduced response. It is less probable that the activation gating variable (m) will cross the threshold required to activate sodium channels for initiating the depolarization phase of the action potential. A slower decline in the sodium inactivation variable (h) is also seen, indicating that sodium channels remain inactivated for an extended duration. Furthermore, as seen in Fig.5.25, the potassium activation variable (n)

grows more slowly, delaying the repolarization phase and the return to the resting potential further contributing to the hypoexcitation, delayed response and prolonged refractory period. Moreover, incorporating the rescue protein mechanism into the model for model for rescue coefficient (k_{Rescue})=1, also shows that the rescue mechanism fails to mitigate the effect of genetic mutation as evident from the fact that the rescue plot and the mutated plot overlap each other (green and red plots).

The plots for the ionic currents of potassium, sodium, and leakage ions with time for the non-mutated (original), mutated and rescue situations are shown in Fig. 5.26. As seen in Fig. 5.26(a), the peak value of the sodium current in the mutated situation is lower than in the non-mutated scenario. This is because when a mutation results in a negative voltage shift, sodium channels find it extremely difficult to get activated and as a result, the voltage threshold for activation is shifted, and fewer channels open at any given membrane potential. As a result, there is less depolarization due to a smaller peak sodium current resulting in hypoexcitation like situation. From Fig.5.26(b), it can be seen that a negative voltage shift also results in a lowered potassium current, which is related to the decreased depolarization caused by the lower sodium current. Since the membrane potential does not reach to the same heights as it did in the non-mutated (original) scenario, fewer potassium channels are activated, resulting in a reduced peak potassium current. This decreased potassium current further explains the lack of numerous spikes, since there isn't enough ionic dynamics present overall to generate additional spikes. Fig.5.26(c) also shows a similar trend for the leakage current owing to a negative voltage shift to the rate constant parameters. Fig.5.26 demonstrates the way a mutation-induced negative voltage shift alters the behaviour of potassium and sodium currents altering the structure and shape of the action potential spike train. Furthermore, incorporation of the rescue mechanism for rescue coefficient (k_{Rescue}) =1 also suggests the failure of the rescue mechanism to restore the ionic currents back into its non-mutated (original) form which is evident from Fig.5.26 as the rescue plot overlaps with the mutated plot as the rescue plot overlaps with the mutated plot (green and red plots).

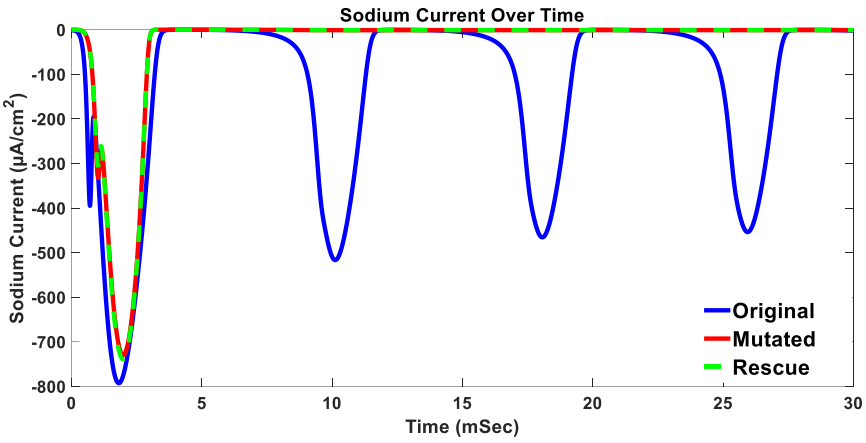

(a)

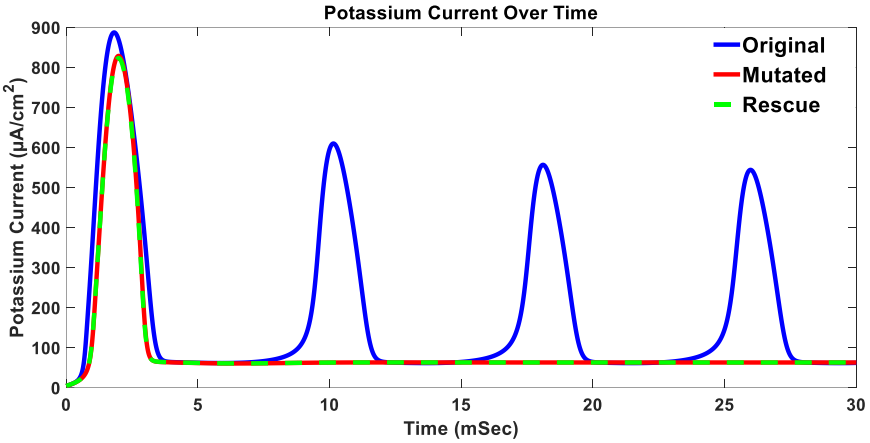

(b)

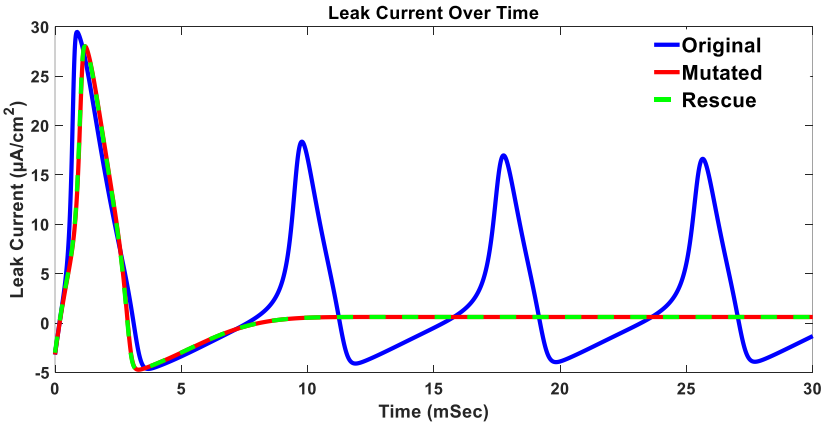

(c)

Fig.5.26 Variation in ionic currents for non-mutated (original), mutated and Rescue (k_{Rescue}=1) conditions over time for -10 mV voltage shift in rate constant (a). For Sodium current (b). For Potassium current (c). For Leakage current

Fig.5.27 illustrates the phase plane plot of the membrane potential (V) against the sodium activation variable (m) for the non-mutated (original), mutated and the rescue scenarios. The plot displays the dynamic interaction between the two variables throughout the action potential

at a negative voltage shift to the rate constant parameters. The phase plane plot shown in Fig.5.27 shows a reduced size and altered shape of the loop which is an indicative of hypoexcitation and a reduced amplitude. The compressed trajectory indicates that the sodium channel activity is substantially suppressed, which reduces the neuron's capacity to generate and sustain action potential. This shows how slight changes to the rate constants that affect the voltage dependence of the gating variables (m, n, and h), may have a significant effect on how neuronal behaviour. The slowly rising sodium activation variable (m) and membrane potential (V) result in a smaller and less dynamic loop and a more substantial depolarization is required to activate the sodium channels. The hypoexcitation condition is also indicated by the delayed rise and decreased slope, which cause the neuron to take longer to cross the threshold needed to initiate an action potential, thereby prolonging the refractory period. The neuron appears to be reacting to stimuli more slowly due to the longer and slower propagation of this delay. The phase plane plot also substantiates the observations made from the previous results that the rescue mechanism fails to counter the effect of genetic mutation for rescue coefficient (k_{Rescue}) =1 as the rescue plot overlaps with the mutated plot (green and red plots) suggesting that the effect of genetic mutation dominates the rescue protein mechanism.

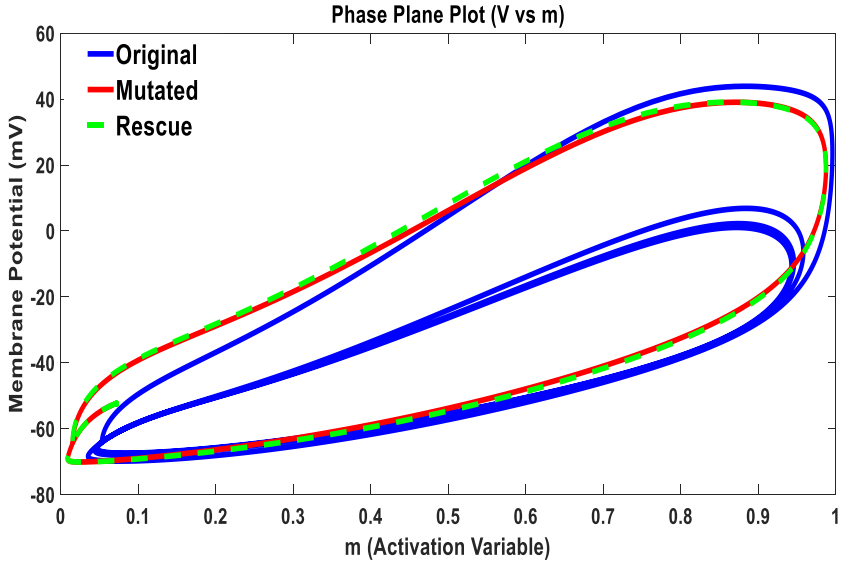

Fig.5.27 Phase plane plot (V vs m) for -10 mV voltage shift in rate constant for non-mutated (original), mutated and Rescue (k_{Rescue}=1) scenarios

D.2 For Rescue coefficient (k_{Rescue})=0

In this section, the rescue protein mechanism is applied in the form of the rescue protein voltage $R_p(V_m)$, shown in Eq.5.14 for a mutated scenario which led to a negative voltage shift (-10 mV) to the rate constant parameters (α, β) and for rescue coefficient (k_{Rescue})=0. The membrane potential plot over time for the original (non-mutated), mutated and rescue scenarios is displayed in Fig. 5.28.

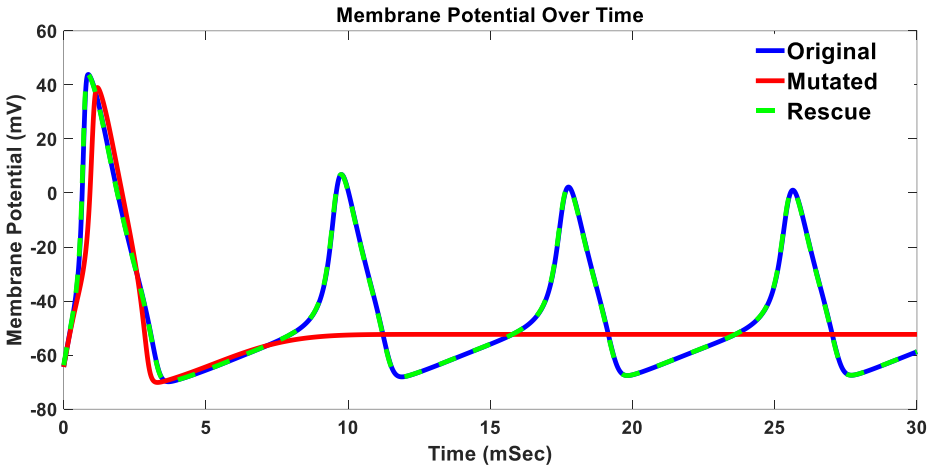

Fig.5.28 Non-mutated (original), mutated and Rescue (k_{Rescue}=0) membrane potential over time for -10 mV voltage shift in rate constant

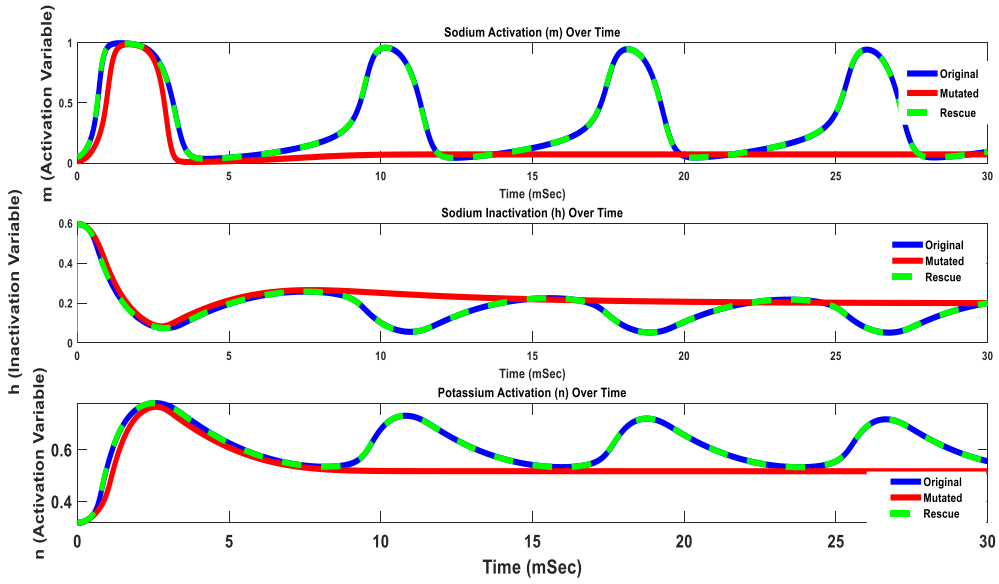

Fig.5.29 Non-mutated (original), mutated and Rescue (k_{Rescue}=0) gating variables over time for -10 mV voltage shift in rate constant

When the rescue coefficient (k_{Rescue}) is 0, observing Fig.5.28 it can be seen that the effect of genetic mutation of ion channels gets completely nullified and the membrane potential returns to its initial non-mutated condition which is evident from Fig.5.28 as the rescue plot

overlaps with the non-mutated (original) plot (green and blue plots) suggesting that the proposed mechanism has successfully managed to mitigate the impact of genetic mutation of ion channels and the normal neuronal excitation is restored. This is also evident by observing the plots for the gating variables (m, n, and h) for non-mutated (original), mutated and rescue scenarios shown in Fig.5.29 where the mutated plot overlaps with the original non-mutated plot (green and blue plots). Thus, the proposed mechanism effectively manages to replicate the complete restoration of the neuronal excitation by mitigating the effect of genetic mutation of the ion channels.

Figs 5.30(a), 5.30(b), and 5.30(c) shows the plots when the rescue protein mechanism applied to the sodium, potassium and leakage currents for recue coefficient (k_{Rescue}) = 0. Observing Fig.5.30, it can be deduced that the rescue plot has successfully been able to mitigate the impact of genetic mutation of ion channels that led to a negative voltage shift to the rate constant parameters as the rescue curve has completely overlapped with the non-mutated (original) plot (green and blue plots), thus restoring back the ionic currents to its original state. This observation has been further substantiated by the phase plane plot as shown in Fig.5.31 where application of rescue coefficient (k_{Rescue}) = 0 causes the mutated scenario to restore back to the original form suggesting that the normal neuronal excitation is restored effectively.

Delays in reaction like this might be a sign of conditions of some form of channelopathies, related to ion channel malfunction occurs. These conditions are often associated with mutations in genes such as KCNQ2, KCNA1, and KCNA2 which are essential for proper ion channel functioning. The altered channel dynamics may cause prolonged refractory periods, prolonged recovery times, and a delayed onset of action potentials.

The critical parameter known as the rescue coefficient (k_{Rescue}) needs to be between 0 and 1 for rescue to occur or not occur at all. The rescue protein mechanism functions as a gradient between two extremes i.e., complete rescue and no rescue. The model makes sure that there is a smooth transition between the non-mutated (original) and mutated states by maintaining k_{Rescue} within this range.

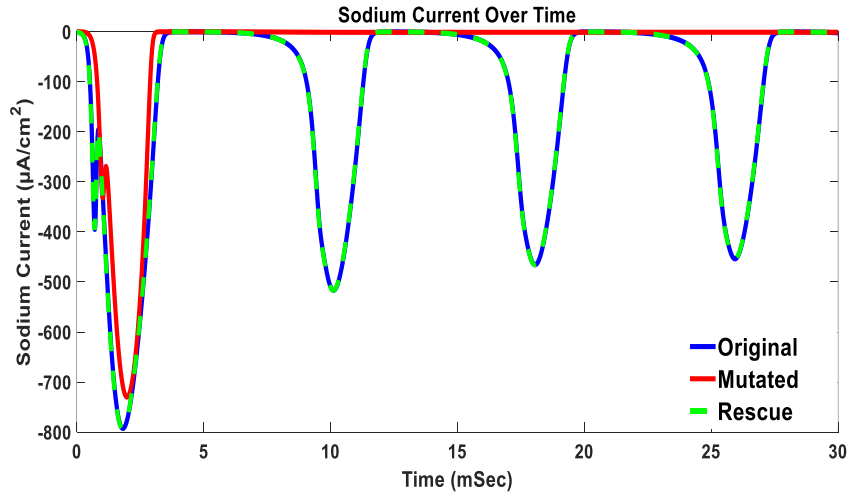

(a)

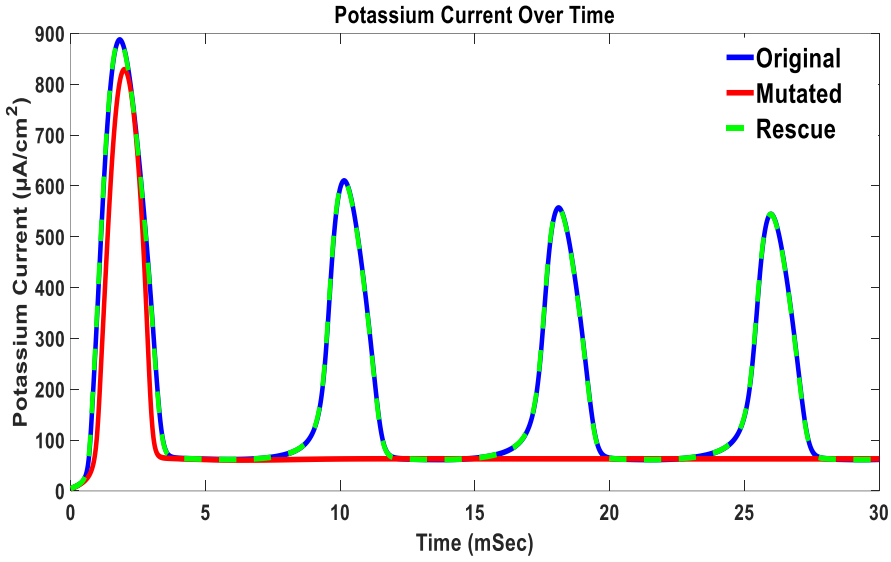

(b)

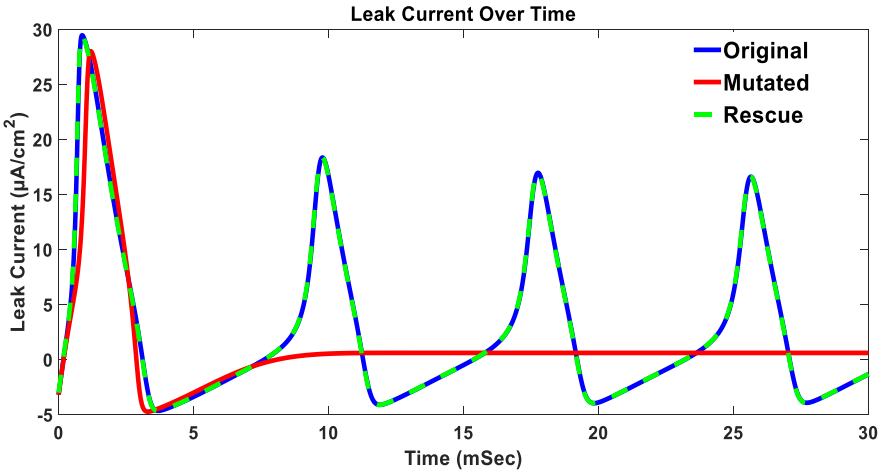

(c)

Fig.5.30 Variation in ionic currents for non-mutated (original), mutated and Rescue (k_{Rescue}=0) conditions over time for -10 mV voltage shift in rate constant (a). For Sodium current (b). For Potassium current (c). For Leakage current

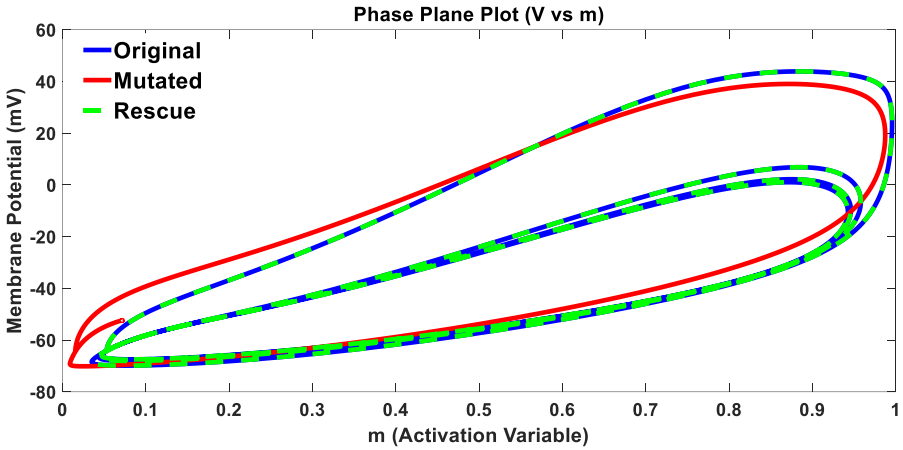

Fig.5.31 Phase plane plot (V vs m) for -10 mV voltage shift in rate constant for non-mutated (original), mutated and Rescue (k_{Rescue}=0) scenarios

k_{Rescue} =1, denotes that the rescue operation has failed, and the effect of mutation dominates the neuronal excitation. On the other hand, the rescue mechanism operates at maximum efficiency when k_{Rescue} =0, completely returning the system to its initial, non-mutated condition. This denotes total recovery or rescue, in which the effect of mutation is completely eliminated. A partial restoration to the non-mutated state is possible by adjusting the rescue coefficient between 1 and 0, which depends on the degree or severity of the genetic mutation. The model is flexible enough to mimic varying degrees of rescue through tuning the value of k_{Rescue} reflecting the possible effectiveness of therapeutic treatments. The comparison Table for the proposed work is enlisted in Table 5.2.

Comparison Table:

Table 5.2: Comparison Table for the current finding with the existing literatures

Work	Methods Used	Results	Remarks
Cintrón-Colón, A. F., Almeida-Alves, G., VanGyseghem, J. M., & Spitsbergen, J. M. (2022). GDNF to the rescue: GDNF delivery effects on motor neurons and nerves, and muscle re-innervation	Rats with peripheral nerve injuries were given electrical muscle stimulation (EMS) in order to assess functional reinnervation using electromyographic recordings and examine the amounts of GDNF mRNA in muscle and nerve tissues, with an	After peripheral nerve injuries, GDNF, a rescue protein, greatly increases motor neurone survival and differentiation, promoting nerve regeneration. RET receptor activation and	The paper does not involve proposing a mathematical equation explicitly for Rescue protein mechanism.

after peripheral nerve injuries. *Neural Regeneration Research*, *17*(4), 748-753.	emphasis on its involvement in nerve regeneration.	related signalling pathways drive this action, underscoring GDNF's pivotal function in nerve healing processes.	
Li, J., Parker, B., Martyn, C., Natarajan, C., & Guo, J. (2013). The PMP22 gene and its related diseases. *Molecular neurobiology*, *47*, 673-698.	Using autophagy modulation and protein aggregation analysis, the study examined how PMP22 mutations affected Schwann cells and peripheral nerves in mutant animals. Understanding the processes behind PMP22-related neuropathies and investigating new treatment approaches to restore compromised nerve functions were the goals of the study.	Enhancing autophagy can help prevent peripheral neuropathies caused by protein misfolding and aggregation caused by mutations in the peripheral myelin protein 22 (PMP22). The study also demonstrates how PMP22 interacts with proteins linked to apoptosis to mediate neuronal cell death.	The paper does not involve proposing a mathematical equation explicitly for Rescue protein mechanism.
Jones, J. I., Costa, C. J., Cooney, C., Goldberg, D. C., Ponticiello, M., Cohen, M. W., ... & Willis, D. E. (2021). Failure to upregulate the RNA binding protein ZBP after injury leads to impaired regeneration in a rodent model of diabetic peripheral neuropathy. *Frontiers in Molecular Neuroscience*, *14*, 728163.	Reverse transcription is used to generate cDNA libraries and isolate RNA. Real-time PCR is then used to analyse gene expression, and immunostaining is used to identify proteins in nerve tissues. The primary investigation of the paper involves investigating the function of rescue proteins in axonal regeneration and the effects of diabetes on mRNA transport and local translation in neurons.	The Rescue protein mechanism is necessary for local mRNA translation in axonal regeneration which is necessary for nerve repair. The disruption of this pathway in diabetes circumstances impairs the translation and distribution of mRNA, hence impeding nerve regeneration.	The paper does not involve proposing a mathematical equation explicitly for Rescue protein mechanism.

Pietrucha-Dutczak, M., Smedowski, A., Liu, X., Matuszek, I., Varjosalo, M., & Lewin-Kowalik, J. (2017). Candidate proteins from predegenerated nerve exert time-specific protection of retinal ganglion cells in glaucoma. *Scientific Reports*, *7*(1), 14540.	The study employed ex vivo retinal explant culture for neuroprotection screening of metallothionein 2 (MT2), in addition to gene ontology (GO) enrichment analysis to evaluate biological processes and functions and proteomic analysis to find enriched proteins.	The study highlights the neuroprotective effect of metallothionein 2 (MT2) in glaucomatous circumstances and shows that certain RNA-binding proteins, intracellular antioxidants, and growth factors are essential for cell survival and regeneration. Furthermore, gene ontology analysis showed that oxidative stress response proteins are more abundant in short-term predegenerated nerve extracts than in long-term predegenerated extracts.	The paper does not involve proposing a mathematical equation explicitly for Rescue protein mechanism.
Current work	**The work involves proposing a robust yet simpler mathematical equation for Rescue protein mechanism of nerve**	**The mathematical relation proposed manages to show the extent of rescue achieved**	**-**

5.6 Summary and Future Remarks

The current work involves putting forward a mathematical framework that provides a simplistic and robust mathematical expression of the membrane potential of nerve incorporating the fundamental parameters of the ECS in order to have a holistic approach for studying neuronal signal generation and transmission.

The first part of the study involves understanding how injury (disease) to the nerve fiber that alters the opening and closing of the ion channels affects neuronal signal under the effect of the ECS of varying sizes. The study shows that the generation and propagation of neuronal signals for both healthy and injured nerves are significantly influenced by the size of the ECS. Additionally, it is implied that there has to be a certain combination of the size of the ECS and the degree of neuronal damage for the nerve signal to propagate without distortion which needs to be further investigated. In the second part, the effect of genetic mutation on the ion channels of nerve is examined and a rescue protein mechanism is put forward which could reverse the effect of these genetic mutations.

The first part of the chapter shows that the generation and propagation of neuronal signals across both healthy and injured nerves are significantly influenced by the size of the ECS. Additionally, for the nerve signal to travel without distortion, there has to be a certain combination of the size of the ECS and the degree of the neuronal damage which needs to be further investigated. Therefore, to comprehend the underlying cause of various neuronal abnormalities associated with hypoexcitation of the neuronal signal such as peripheral neuropathy, Guillain-Barré syndrome, Charcot-Marie-Tooth condition, etc., as well as conditions symbolic of hyperexcitation such as epilepsy, seizures, etc., a thorough examination of the ECS and its function in neuronal signal transmission is essential. Furthermore, comprehending how the ECS affects neural impulses may aid in a better understanding of conditions like ischemia, trauma, etc. Thus, it may be inferred that the ECS plays a much deeper role in governing neuronal signals. It is known that the ECS is essential for the distribution of chemotherapeutic drugs therefore, the proposed framework, with its simple membrane potential expression given in Eq.5.13, may prove useful in this regard. It might also help in the diagnosis, prediction, and understanding of different neurological conditions impacted by ECS of different sizes.

In the second part of the chapter, an attempt has been made to mimic the effects of genetic mutations that are known to change how ion channels function by inducing voltage shift to the rate constant (α and β) parameters, which would eventually change the gating variables of the ion channels and have proposed a rescue protein mechanism that could alter the effect of these mutations. The aim of this study is to understand how both positive and negative voltage shifts to the rate constant parameters affects neuronal excitation, which would contribute to the existing understanding of how small changes in channel behaviour can have significant physiological effects by affecting gating variables, ionic currents, and the membrane

potential. This study is intended in aiding in the development of targeted therapies and interventions for associated medical disorders.

The findings indicate that a hyperexcitable condition which is characterised by a greater firing frequency and a larger peak amplitude is brought on by a positive voltage shift to the rate constant parameters. This is caused due to the sodium channel variable (m) activating more quickly and also by the faster activation of the potassium activation variable (n) thereby speeding up the repolarization process. A negative voltage shift, on the other hand results in a hypoexcitable state which delays and weakens action potential. The inability of the sodium channels to open results in a delayed depolarization and smaller action potential amplitudes. In addition to responding more slowly, the potassium activation variable (n) also prolongs the refractory period and the repolarization phase and as a result, there is a decrease in potassium and sodium currents, which adds to the overall hypoexcitation.

Mutations in sodium channel genes (e.g., SCN1A, SCN2A, and SCN8A) have significance in disorders like epilepsy, where a positive voltage shift leading to hyperexcitation is associated. Conversely, the hypoexcitation resulting from a negative voltage shift to the rate constants is associated with genetic mutations of potassium channels (e.g., KCNA's, KCNQ2, KCNJ2) and sodium channels (e.g., SCN4A), which are characterised by delayed responses and longer refractory periods, this implies that there must be a limit to the degree of mutation at which the signal maintains its integrity without deforming from its original form which is to be further investigated.

The rescue protein mechanism which has been incorporated into the proposed framework in the form of a rescue protein voltage $R_p(V_m)$ is assumed to be a combination of the original and the mutated membrane potential. The rescue coefficient k_{Rescue} acts as a tuning parameter that regulates how much a rescue protein mechanism counteracts the effects of a mutation. When $k_{Rescue}= 1$ the rescue protein voltage $R_p(V_m)$ becomes exactly same as the mutated voltage ($V_{m,mutated}$) suggesting that there is no rescue taking place and the rescue mechanism fails to counter the effect of mutation and when $k_{Rescue}= 0$, where the rescue protein voltage $R_p(V_m)$ becomes exactly same as the non-mutated (original) voltage ($V_{m,Original}$), where the dynamics of the membrane potential revert to their non-mutated (normal) condition suggesting that the rescue protein mechanism has fully managed to revert back or mitigate the effect of genetic mutation.

The rescue coefficient, or k_{Rescue} should so be calculated that, depending on the extent of the rescue, its value should range from 0 to 1. Precise control over the extent to which the rescue protein corrects for the mutation is made possible through tuning the value of k_{Rescue}. Thus, a detailed examination of the rescue protein mechanism and its potential operation in many scenarios is made possible by this rescue coefficient. Given its adaptive nature, k_{Rescue} ought to be a vital source for investigating the range of potential outcomes of rescue proteins and understanding their capacity to re-establish regular neuronal activity. Conversely, if membrane potential for the non-mutated (original) state, mutated state and the drug induced rescue state could be calculated experimentally, then the value of the rescue coefficient could be obtained which would show how much the drug has been able to mitigate the impact of genetic mutation of ion channels with a value close to 1 indicating less effectiveness of the drug to mitigate the impact of mutation and a value close to 0 indicating that the drug has shown signs of mitigating the impact of these mutations. Thus, the proposed rescue protein mechanism would provide pathway which that would aid in therapeutic treatments such as quantifying drug efficacy, predicting long term drug effects, optimization of drug dosage comparing different treatments etc.

The proposed framework offers a reliable and comprehensive method for studying neuronal signals by including the fundamental ECS characteristics into a membrane potential expression. The suggested framework also manages to mimic the activity of a real nerve fiber in terms of responses, showing its efficacy while requiring less mathematical and computational complexity and producing results quickly. Since the ECS is known to have an influence on neural behaviour, the proposed framework could also provide insight about the role of the ECS in governing neuronal excitability. Furthermore, the rescue protein mechanism that has been proposed in this work would provide further insights towards development of therapeutic treatments of various neurological conditions and also to understand the causes of various ion channel mutations.

Publications:

Journal:

1. **Das, B.,** Baruah, S. M. B., Singh, S., & Roy, S., “Insights into Nerve Signal Propagation: The Effect of Extracellular Space in Governing Neuronal Signal for healthy and injured Nerve Fiber using Modified Cable Model”, Journal name (Journal of Electronics, Electromedical Engineering, and Medical Informatics), Vol. 6, no. 2,

pp. 206-218, 2024, DOI: https://doi.org/10.35882/jeeemi.v6i2.394 . (Scopus (e-ISSN: 2656-8632)).

2. **Das, B.,** Baruah, S. M. B., & Roy, S., "A Modelling and Simulation Framework for Integrating Rescue Protein Mechanism for Neuronal Excitation Recovery", Journal name (International Journal of Bioinformatics Research and Applications), Inderscience Publishers (Scopus (ISSN: 1744-5485)), (Under Review).